Results

Analysis of genome-wide DNA methylation

Human iPS cell lines (MRC-iPS [13] and AM-iPS cell lines [12]) independently established in our laboratory by retroviral infection of 4 genes (*OCT-3/4*, *SOX2*, *c-MYC*, and *KLF4*), based on the Yamanaka's pioneer protocols [2] from 2 fully differentiated cells (MRC-5, fetal lung fibroblast cells, and AM936EP, amnion cells), were used as a primary source for experimentation (Table 1). These cells clearly showed human iPS characters [12,13].

To examine DNA methylation status in six iPS, two ES [14], and eight differentiated cell lines (Table 1), we therefore examined genome-wide DNA methylation using Illumina's Infinium HumanMethylation27 BeadChip, on which oligonucleotides for 27,578 CpG sites covering more than 14,000 genes are mounted, mostly selected from promoter regions. This assay system provides advantageous quantitative measurement. DNA methylation levels were recorded using a scoring system ranging from "0" (completely unmethylated) to "1" (fully-methylated). Using multiple repetitions, we analyzed 24,949 out of 27,578 CpG sites with 16 samples (see Materials and Methods), categorizing them into three groups; Low (score≤0.3), Middle (0.3<score≤0.7), or High (0.7<score) methylation. Overall, methylation levels in pluripotent stem cells and differentiated cells are shown in Fig. 1A, with the levels in each cell line presented in Table S1. While the percentage of the High class in differentiated cells was 16.3% on average, the percentage in iPS/ES cells was 25.3% (Fig. 1A). The number of CpG sites categorized in the High class is significantly greater in pluripotent stem cells compared with differentiated cells. Hierarchical clustering analysis clearly discriminates iPS/ES cells from the differentiated cells (Fig. 1B). Hyper-methylated sites (shown in red) are widespread in the heat map in iPS/ES cells, compared with the differentiated cells (Fig. 1B), suggesting that gene promoters in iPS/ES cells are hyper-methylated, compared with those in differentiated cells.

About two-thirds of the CpG sites were at a Low methylated level in both iPS/ES cell and differentiated cell groups (Fig. 1A and B). Another computation found 13,971 CpG sites to consistently show a score of lower than 0.3. This suggests that a significant fraction of the CpG sites examined may have less involvement in methylation, although some might become methylated under different conditions. As most CpG sites on the chip were chosen simply based on the location in promoters, it is possible that some CpG sites may be positioned at a distance from the target site, even in a promoter controlled by DNA methylation. Analysis of our and all published data indicated that a group of CpG sites more suitable to methylation analyses could be identified, allowing us to focus attention on specific changes in methylation levels seen between iPS/ES and differentiated cells.

Differentially methylated site (DMS) in the promoters. Firstly, we defined the "differentially methylated site" (DMS), representing a CpG site whose score differed 0.3 points and more between the two cell groups. The DMSs between MRC-iPS and AM-iPS cells, and also between iPS and ES cells, were only 1.0% and 2.8% of all the CpG sites, respectively (Fig. 1C), suggesting that iPS and ES cells have similar methylation status. In contrast, the DMSs between AM936EP and AM-iPS cells, and between MRC-5 and MRC-iPS cells, were 11.3% and 10.6%, respectively, suggesting that iPS cells and their parental cells have differentially methylated status (Fig. 1C and D). It should be noted that approximately 80% of the DMSs between the iPS cells and their parental cells changed to a "hyper-methylated" state from a "hypo-methylated" state in iPS cells (Fig. 1C). Comparison of DMSs between AM- and MRC-iPS cells, and between iPS and ES cells show slight but significant difference (Fig. 1C). In 261 DMSs between MRC- and AM-iPS cells (MA-DMSs), 203 sites in AM-iPS cells and 165 in MRC-iPS cells showed no difference from their parental cells, suggesting that these sites in iPS cells are inherited from their tissue origin (Fig. 1E). In addition, 414 out of 694 DMSs between MRC-iPS and ES cells (ME-DMSs) and 581 out of 990 DMSs between AM-iPS and ES cells (AE-DMSs) are inherited DMSs (Fig. 1E). Interestingly, approximately 40% of DMSs between iPS and ES cells are iPS-specific DMSs, meaning that these sites are aberrant methylated in iPS cells (Fig. 1E). In

Table 1. A list of human cells analyzed for a methylation state in this study.

Cell ID	Description	ability of differentiation
MRC5	Fetal lung fibroblast cells	None
MRC-iPS-11	MRC5-derived iPS cells (P4)	Pluripotent
MRC-iPS-19	MRC5-derived iPS cells (P4)	Pluripotent
MRC-iPS-75	MRC5-derived iPS cells (P4)	Pluripotent
AM936EP	Amnion-derived cells (P6)	None
AM-iPS-3	AM936EP -derived iPS cells (P4)	Pluripotent
AM-iPS-6	AM936EP -derived iPS cells (P4)	Pluripotent
AM-iPS-8	AM936EP -derived iPS cells (P4)	Pluripotent
UtE1104	Endometrium-derived cells (P7)	None
H4-1	Bone marrow stroma-derived cells (P26)	None
Mim1508E	Auricular cartilage-derived cells (P1)	Cartilage
Yub636BM	Extra finger bone marrow-derived cells (P3)	Bone
PAE551	Placental artery endothelial cells (P13)	None
Edom22	Menstrual blood-derived cells (P1)	Myoblast
HUES3	Embryonic stem cells (P29)	Pluripotent
HUES8	Embryonic stem cells (P24)	Pluripotent

Numbers in parenthesis with P indicate passage in culture on the cells used in the methylation analysis.
doi:10.1371/journal.pone.0013017.t001

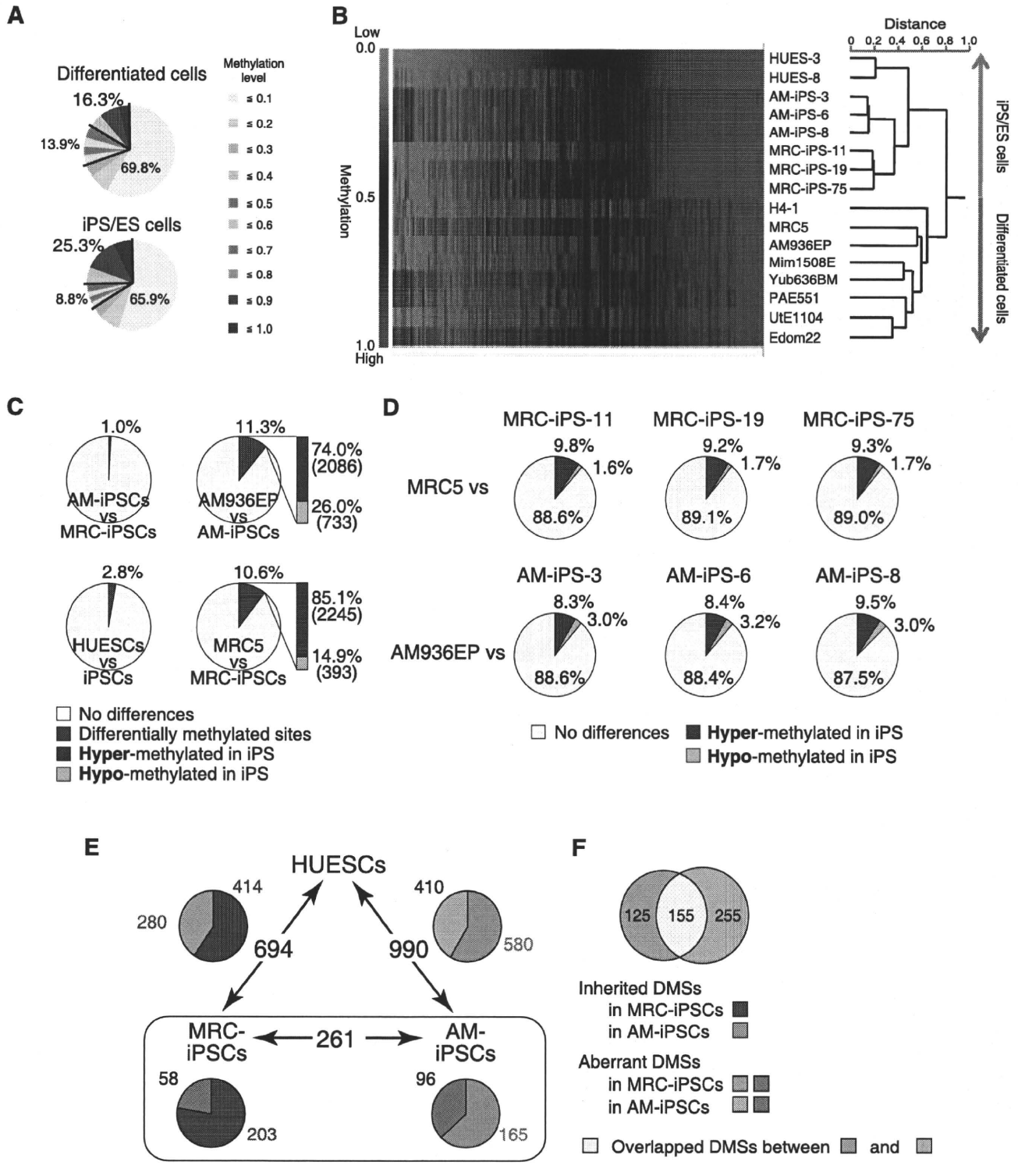

Figure 1. The ratio of hyper-methylated sites in iPS/ES cells was significantly larger than that of the differentiated cells. (**A**) Ratio of Low (methylation score≤0.3), Middle (0.3<score≤0.7), and High (0.7<score) methylated states in 24,949 CpG sites. (**B**) Clustering analysis. Heat map showing hyper-methylation in human iPS/ES cells compared with differentiated cells. The Heat map in hierarchical clustering analysis represented DNA methylation levels from completely methylated (red) to unmethylated (green). Epigenetic distances (Euclidean Distance) were calculated by NIA Array. (**C**) Comparisons of CpG sites between two groups show high similarities between AM-iPS and MRC-iPS cells or between human ES cells (HUESCs) and iPS cells (iPSCs). In contrast, 11.3% and 10.6% of CpG sites are differentially methylated in AM-iPS and MRC-iPS cells, respectively, compared to their parental cells (AM936EP and MRC5). It should be noted that 74.0% and 85.1% of the differentially methylated sites (DMSs) are hyper-methylated in AM-iPS and MRC-iPS cells, respectively, compared to their parental cells. (**D**) Comparison of the 24,949 CpG sites between iPS cells and their parental cells. (**E**) DMSs among human ES cells, AM- and MRC-iPS cells. The relative amount of inherited/aberrant DMSs is indicated in the pie chart. (**F**) Overlapped aberrant DMSs between MRC- and AM-iPS cells.
doi:10.1371/journal.pone.0013017.g001

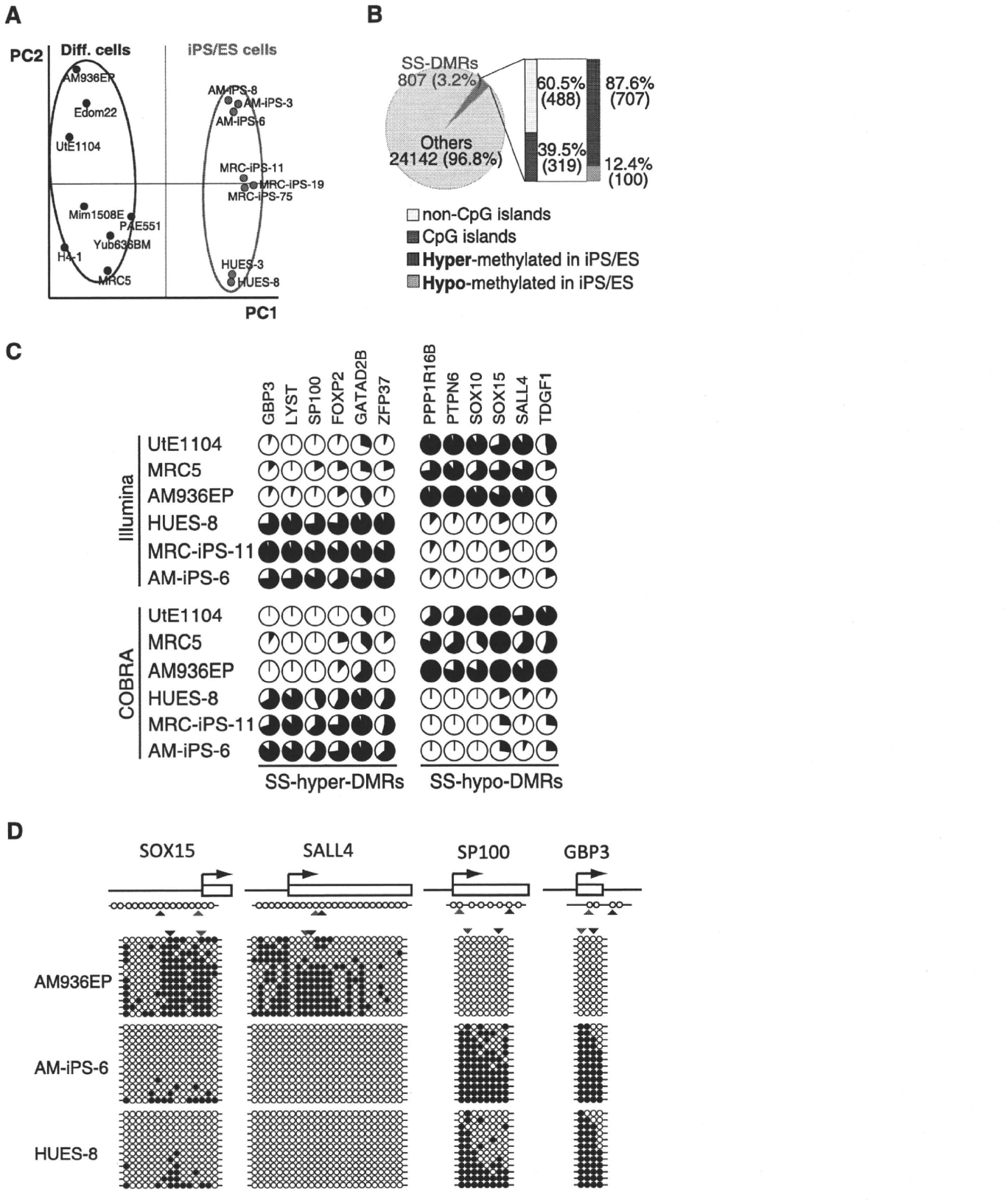

Figure 2. Pluripotent stem cells are significantly more hyper-methylated than differentiated cells. (**A**) Principal component analysis (PCA) for DNA methylation states of 24,949 CpG sites with 16 human cell lines. The PC1 axis clearly distinguish iPS/ES cell group from differentiated cells, while human iPS cells are very close to human ES cells. (**B**) Stem cell-specific differently methylated regions (SS-DMRs) were defined by PC1. In the pluripotent stem cells, 60.5% of the SS-DMRs are located outside of CpG islands and 87.6% of the SS-DMRs are hyper-methylated. (**C**) DNA methylation levels at promoter regions in 12 representative genes determined by Illumina Infinium HumanMethylation27 assay and Bio-COBRA.

Details of these genes are described in Table S6B. The promoter regions of these genes were defined as the SS-DMRs. The relative amount of methylated DNA ratio is indicated as the black area in the pie chart. The same methylation patterns in 12 regions were detected both by Infinium assay and COBRA. (**D**) Bisulfite sequencing analysis of the same regions that were analyzed by Infinium assay and COBRA assay in *SOX15*, *SALL4*, *SP100* and *GBP3*. (Top) Schematic diagram of the genes. Arrows, open boxes and open circles represent transcription start site, first exon and position of CpG sites, respectively. (Bottom) Open and closed circles indicate unmethylated and methylated states, respectively. Red and blue arrowheads represent the position of CpG sites in Infinium assay and COBRA, respectively.
doi:10.1371/journal.pone.0013017.g002

aberrant DMSs, 155 sites overlapped between MRC- and AM-iPS cells (Fig. 1F and data set S1, S2, S3). Overlapping aberrant DMSs are located at promoters in genes such as gene for FZD10, MMP9 and three zinc finger proteins (ZNF551, ZNF513 and ZNF540). These genes are hyper-methylated in iPS cells than parental cells and ES cells. Approximately 80% of aberrant DMSs are hyper-methylated, compared with parent cells and ES cells.

Defining stem cell specific differentially methylated regions (SS-DMRs). Principal component analysis (PCA) shows high similarity among human iPS and ES cells and clearly separates the iPS/ES cells from the differentiated cells, which is supported by hierarchical clustering analysis (Fig. 1B and Fig. 2A). Based on principal component 1 (PC1), 807 (3.2%) out of 24,949 sites were deduced to change their methylation state along with "stemness" (Fig. 2B). We designated a region represented by such CpG sites as "stem cell specific differentially methylated regions" (SS-DMRs). Of the 807 SS-DMRs, 39.5% (319 sites) are localized on CpG islands, whereas 60.5% (488 sites) are not (Fig. 2B), although 72.5% CpG sites on the bead-chips occur on CpG islands. Thus, promoter regions on non-CpG islands were more affected during reprogramming towards pluripotent stem cells. 707 sites (87.6%) of the SS-DMRs were significantly increased in the methylation levels in iPS/ES cells, compared with those in the differentiated cells, and we designated these sites as "stem cell specific hyper-differentially methylated regions (SS-hyper-DMRs) " (Fig. 2B and data set S4). In contrast, 100 sites (12.4%) were decreased and designated as "stem cell specific hypo-differentially methylated regions (SS-hypo-DMRs) " (Fig. 2B and data set S5). We also confirmed the methylation state in the promoter regions for some of the detected genes by another means, i.e. quantitative combined bisulfite restriction analysis (COBRA) [15] (Fig. 2C). In addition, results of bisulfite sequencing of the region surrounding the SS-DMRs corresponded to results of Infinium assay and COBRA (Fig. 2D).

Gene ontology analysis with the SS-DMRs. We searched gene ontology databases for details of the SS-DMRs. Interestingly, SS-hypo-DMRs are abundant in genes related to nucleic acid binding and transcription factors, which may function in iPS cells. On the other hands, SS-hyper-DMRs are abundant in genes related to differentiation (Table 2). We also subjected the SS-DMRs to KEGG (Kyoto Encyclopedia of Genes and Genomes) pathway. Cytokine receptor interaction cascade, MAPK signaling, and Neuroactive ligand-receptor interaction are all major keywords for SS-hyper-DMRs (Table S2).

Expression of genes with SS-DMRs in human iPS/ES cells. To address whether changes in DNA methylation state are associated with expression levels, we surveyed genes showing more than 5-fold change of expression in human iPS/ES cells, compared with those in differentiated cells, using the GEO database [16,17]. Twenty-three genes represented by SS-hypo-DMRs were found in "genes significantly expressed in iPS/ES cells" (Table 3 and Table S3A). Representative genes, including *SOX15*, *SALL4*, *TDGF1*, *PPP1R16B* and *SOX10*, are expressed with hypo-methylation states in iPS/ES cells (Fig. 3A). On the other hand, forty-three genes represented by SS-hyper-DMRs were found in "genes significantly suppressed in iPS/ES cells" (Table S3B and S4). Representative genes, *SP100* and *GBP3*, are suppressed by hyper-methylation in iPS/ES cells (Fig. 3A). Among DNA methyltransferases, *DNMT3B* was reported to be highly expressed in human ES cells [18]. *DNMT3A*, *DNMT3B* and *DNMT3L* were indeed expressed in iPS/ES cells (Fig. 3A). The *DNMT3A* promoter in iPS/ES cells became demethylated, while *DNMT3B* and *DNMT3L* promoters remained low methylated during reprogramming (Fig. 3A and Table S5A), leading us to analyze chromatin in iPS/ES cells in addition to DNA methylation.

Histone H3K4 and H3K27 modification of genes with the SS-DMRs. Histone modification is another important mechanism in epigenetics. Methylation of lysine 4 (K4) and 27 (K27) on histone H3 is associated with active and silent gene expression, respectively [19], while bivalent trimethylation (me3) of H3K4 and K27 represses their gene expression in ES cells [20,21]. Based on the database of the UCSC Genome Bioinformatics, the promoter of *DNMT3B* in human ES cells is highly modified by 3K4me3, compared with that in human lung fibroblasts (Table S5B). No differences in histone modification of H3K4me3 or H3K27me3 between ES and lung fibroblasts at promoter of *DNMT3L* were detected (Table S5B). We also compared DNA methylation of the SS-DMRs with reported data for whole-genome mapping of H3K4me3 and H3K27me3 in the promoter regions of human ES cells [22]. In SS-hyper-DMRs, 68.8% do not have trimethylation of H3K4 and K27 (Fig. 3B). On the other hand, 42.3%, 1.3%, and 30.8% of SS-hypo-DMRs are marked with H3K4me3, H3K27me3, and bivalent H3K4me3 and K27me3, respectively (Fig. 3B). Thirteen out of the 23 genes in

Table 2. A list of top 7 categories of GO Term in "SS-DMRs".

Molecular Function		
PantherID: GO Term	**Count. Genes**	**%**
SS-hypo-DMRs		
MF00042:Nucleic acid binding	30	41.10%
MF00036:Transcription factor	15	20.55%
MF00099:Small GTPase	11	15.07%
MF00137:Glycosyltransferase	8	10.96%
MF00082:Transporter	6	8.22%
MF00154:Metalloprotease	6	8.22%
MF00098:Large G-protein	6	8.22%
SS-hyper-DMRs		
MF00213:Non-receptor serine/threonine protein kinase	124	20.98%
MF00262:Non-motor actin binding protein	119	20.14%
MF00001:Receptor	80	13.54%
MF00131:Transferase	76	12.86%
MF00099:Small GTPase	66	11.17%
MF00242:RNA helicase	57	9.64%
MF00261:Actin binding cytoskeletal protein	53	8.97%

doi:10.1371/journal.pone.0013017.t002

Table 3. A list of 23 genes with SS-hypo-DMRs exhibiting 'high' expression in human iPS/ES cells.

TargetID	Gene name	Fold change of expression	DNA methylation level in iPS/ES cells	DNA methylation level in Diff. cells
cg07337598	*ANXA9, annexin A9*	5.53	0.294±0.023	0.712±0.014
cg24183173	*BCOR, BCL-6 interacting corepressor*	5.06	0.014±0.005	0.784±0.051
cg21207436	*C14orf115, hypothetical protein LOC55237*	63.49	0.052±0.005	0.442±0.036
cg22892904	*CBX2, chromobox homolog 2*	11.48	0.068±0.006	0.607±0.051
cg24754277	*DAPK1, death-associated protein kinase 1*	28.34	0.115±0.005	0.708±0.049
cg21629895	*DNMT3A, DNA cytosine methyltransferase 3 alpha*	12.88	0.452±0.011	0.769±0.039
cg02932167	*ECEL1, endothelin converting enzyme-like 1*	17.57	0.115±0.007	0.672±0.059
cg25431974	*ECEL1, endothelin converting enzyme-like 1*	17.57	0.125±0.013	0.674±0.093
cg04515567	*FOXH1, forkhead box H1*	55.88	0.602±0.014	0.855±0.006
cg04464446	*GAL, galanin preproprotein*	194.63	0.241±0.022	0.735±0.056
cg00943909	*GNAS, guanine nucleotide binding protein*	47.33	0.076±0.016	0.528±0.081
cg27661264	*GNAS, guanine nucleotide binding protein*	47.33	0.037±0.005	0.355±0.054
cg18741908	*GPR160, G protein-coupled receptor 160*	60.48	0.068±0.006	0.466±0.038
cg20674521	*KCNJ4, potassium inwardly-rectifying channel J4*	6.11	0.306±0.024	0.772±0.043
cg21129531	*LRRC4, netrin-G1 ligand*	7.04	0.027±0.004	0.788±0.058
cg06144905	*PIPOX, L-pipecolic acid oxidase*	42.97	0.100±0.015	0.558±0.080
cg13083810	*POU5F1, POU domain; class 5;*	559.14	0.563±0.025	0.919±0.009
cg27377213	*PPP1R16B, protein phosphatase 1 regulatory inhibitor subunit 16B*	65.86	0.097±0.009	0.796±0.102
cg19580810	*RAB25, member RAS oncogene family*	6.16	0.062±0.010	0.703±0.030
cg09243900	*RAB25, member RAS oncogene family*	6.16	0.105±0.013	0.595±0.031
cg06303238	*SALL4, sal-like 4*	227.35	0.013±0.005	0.736±0.075
cg06614002	*SOX10, SRY-box 10*	5.23	0.028±0.005	0.829±0.046
cg01029592	*SOX15, SRY-box 15*	10.19	0.174±0.011	0.692±0.032
cg10242476	*TDGF1, teratocarcinoma-derived growth factor 1*	2472.59	0.146±0.013	0.387±0.052
cg20277416	*TM7SF2, transmembrane 7 superfamily member 2*	5.23	0.380±0.017	0.833±0.027
cg05656364	*VAMP8, vesicle-associated membrane protein 8*	9.69	0.070±0.010	0.698±0.081

Fold change of expression: Fold change of expression of the listed gene in human iPS/ES cells against the expression level in differentiated cells.

doi:10.1371/journal.pone.0013017.t003

Table 3 have trimethylation solely on K4 (Fig. 3C). Six genes have no histone trimethylation on K4 and K27 and the rest have bivalent K4/K27 trimethylation (Fig. 3C).

Discussion

Our genome-wide DNA methylation analysis shows that iPS and ES cells have similar methylation status although DNA methylation status of AM-iPS cells was closer to that of MRC-iPS cells than to that of ES cells in a small fraction. Doi et al. reported 71 differential methylated regions covering 64 genes between human iPS cells and ES cells [23]. Comparison of 535 aberrant DMSs (overlapping, 155; MRC-iPS specific, 125; AM-iPS specific, 255) with Doi's data, six genes that are *HOXA9*, *A2BP1*, *FZD10*, *SOX2*, *PTPRT* and *HYPK* overlapped. The inconsistency of most DMSs may be due to the stochastic nature of aberrant methylation through the genome. Human iPS and ES cells have general hyper-methylated status compared with differentiated cells. Our present genome-wide study indicates that pluripotent stem cells are generally hyper-methylated at promoter regions in comparison with differentiated cells. In the SS-DMRs, the number of CpG sites on non-CpG islands is grater than those on CpG islands, suggesting that promoter regions on non-CpG islands were more affected during reprogramming towards pluripotent stem cells. This result is consistent with the suggestion by Fouse et al. (2008) [24] that DNA methylation in mouse ES cells primarily occurred on non-CpG island regions of promoters.

Gene ontology analysis shows that signal transduction and transmembrane are major keywords for SS-hyper-DMRs. Most genes with SS-hyper-DMRs relate to differentiation. Recent studies demonstrate that blocking the p53 and TGFß pathways improves efficiency of generation of iPS cells [25,26,27,28,29,30]. Some genes related to these pathways are included in SS-hyper-DMR. Approximately 70% of SS-hyper-DMR have no modification of H3K4 and H3K27, suggesting that most genes with SS-hyper-DMRs are rigorously turned off by DNA methylation. By combining these findings with the result of *DNMT3A*, *DNMT3B* and *DNMT3L* induction in iPS/ES cells, we suggest that SS-hyper-DMRs apparently include genes that play a role in differentiated cells. Moreover, they must be silenced by DNMTs to establish pluripotency. We then identified 43 genes with SS-hyper-DMRs from "genes significantly suppressed in iPS/ES cells" (Table S3B and S4). In particular, *GBP3* and *SP100* could be used as epigenetic markers for pluripotency.

In addition, we successfully determined 23 genes with SS-hypo-DMRs from "genes significantly expressed in iPS/ES cells" (Table 3 and Table S3A). Those genes may start to be induced by demethylation and a significant subset of genes that act for de-

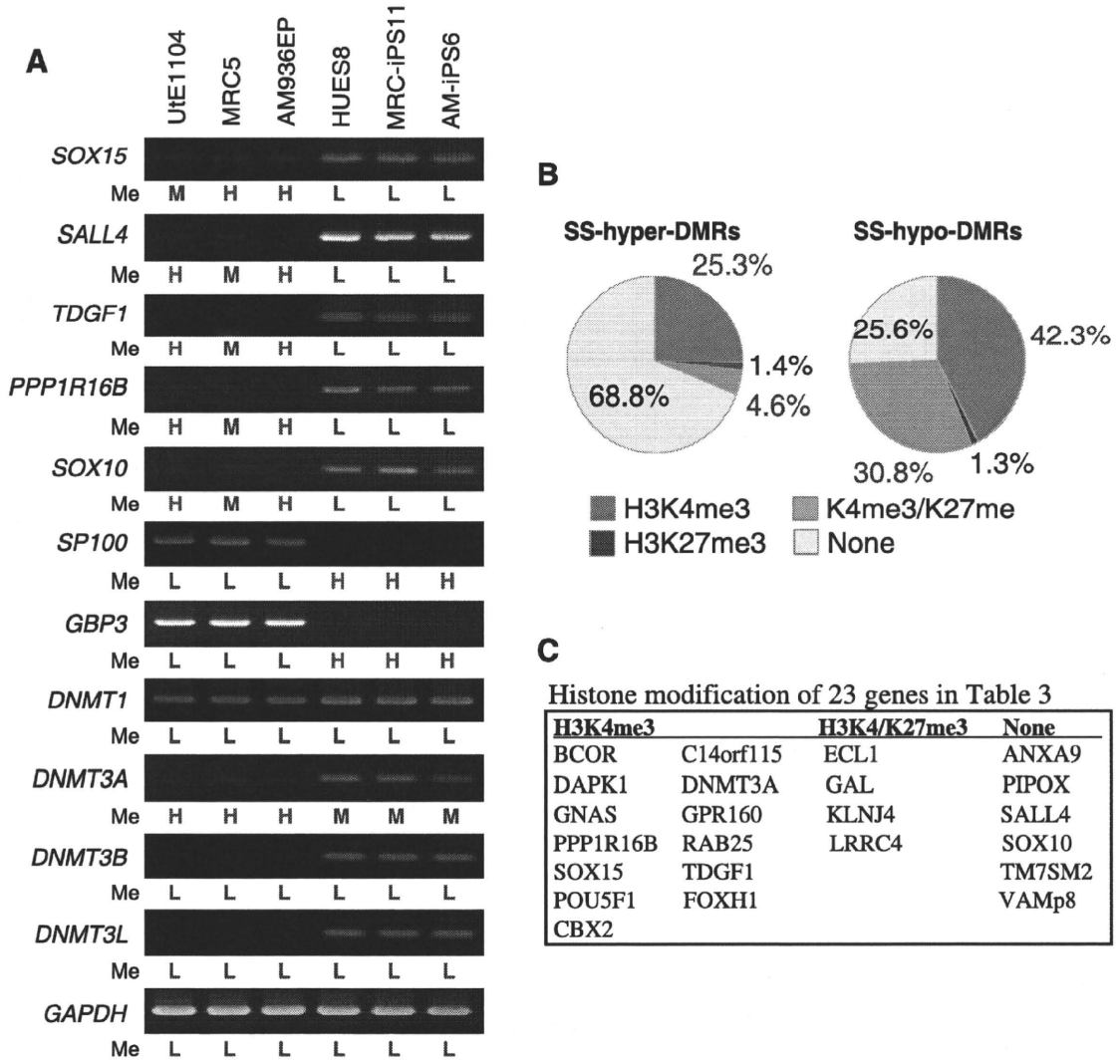

H3K4me3		H3K4/K27me3	None
BCOR	C14orf115	ECL1	ANXA9
DAPK1	DNMT3A	GAL	PIPOX
GNAS	GPR160	KLNJ4	SALL4
PPP1R16B	RAB25	LRRC4	SOX10
SOX15	TDGF1		TM7SM2
POU5F1	FOXH1		VAMp8
CBX2			

Figure 3. Expression and histone modification of the SS-DMRs related genes. (**A**) Expression patterns of representative genes. RT-PCR analysis of 7 representative genes and methyltransferase genes. Methylation levels (Me) of each promoter are shown under each panel. H = High methylation (0.7<score); M = Middle methylation (0.3<score≤0.7); L = Low methylation (score≤0.3). (**B**) Comparable distribution of the SS-DMR and histone trimethylation (me3) of H3K4 and H3K27. Percentage of H3K4me3, H3K27me3, bivalent H3K4me3/K27me3 or non-modification on genes in SS-hyper-DMRs and in SS-hypo-DMRs. (**C**) Histone modification of 23 genes in Table 3.
doi:10.1371/journal.pone.0013017.g003

differentiation escape methylation in pluripotent stem cells during global reprogramming. Promoters of most marker genes expressed in human iPS/ES cells were low methylated in all cells examined (Table S5C). Analysis of histone modification of H3K4me3 and K27me3 from the database suggested that expression of *DNMT3B* might be regulated by methylation of H3K4 but expression of *DNMT3L* might not be under control of histone modification of H3K4me3 and K27me3. Most genes with SS-hypo-DMRs without expression in human iPS/ES cells have modification of H3K4me, bivalent H3K4me/K27me, or none, but do not have H3K27me3 modification. These genes may therefore be ready to be activated upon differentiation.

These findings are in generally consistent with the previous reports that have compared methylation profiles in somatic cells, iPS cells, and ES cells [23,31,32]. However, their analyses were limited only to human fibroblasts as a source for generation of iPS cells. In this study, we analyzed human extra-embryonic amnion cells and iPS cells. The DNA methylation profile at promoter sites clearly distinguished human pluripotent stem cells from differentiated cells. The SS-DMRs defined in this experiment can be used as a signature for "stemness". In addition, knowledge of the DNA methylation profile in human ES and iPS cells derived from different cell types is absolutely imperative and may allow us to screen for optimum iPS/ES cells and to validate and monitor iPS/ES cell derivatives for human therapeutic applications.

Materials and Methods

Human Cells

Human endometrium, bone marrow stroma, auricular cartilage, extra finger bone marrow, amnion, placental artery endothelium and menstrual blood cells were collected by scraping tissues from surgical specimens as a therapy, under signed informed consent, with ethical approval of the Institutional Review Board of the National Institute for Child Health and Development, Japan. Signed informed consent was obtained from

donors, and the surgical specimens were irreversibly de-identified. All experiments handling human cells and tissues were performed in line with Tenets of the Declaration of Helsinki. Endometrium (UtE1104), bone marrow stroma (H4-1) [33], auricular cartilage (Mim1508E), extra finger bone marrow (Yub636BM), amnion (AM936EP), placental artery endothelium (PAE551) and menstrual blood cell (Edom22) [34] cell lines were independently established in our laboratory. H4-1, Mim1508E, Yub636BM, AM936EP, Edom22, and MRC-5 [35] cells were maintained in the POWEREDBY10 medium (MED SHIROTORI CO., Ltd, Tokyo, Japan). PAE551 were cultured in EGM-2MV BulletKit (Lonza, Walkersville, MD, USA) containing 5% FBS. Human induced pluripotent stem (iPS) cells were generated, via procedures described by Yamanaka and colleagues [2] with slight modification. Human iPS cell lines derived from MRC-5 were designated as MRC-iPS cells [13], also iPS cell lines from AM936EP were named as AM-iPS cells [12]. Human iPS cells were maintained in iPSellon medium (Cardio Incorporated, Osaka, Japan) supplemented with 10 ng/ml recombinant human basic fibroblast growth factor (bFGF, Wako Pure Chemical Industries, Ltd., Osaka, Japan). Frozen pellets of human ES cell (HUESCs) were kindly gifted from Drs. C. Cowan and T. Tenzan (Harvard Stem Cell Institute, Harvard University, Cambridge, MA).

Illumina Infinium HumanMethylation27 BeadChip assay

Genomic DNA was extracted from cells using the QIAamp DNA Mini Kit (Qiagen). One microgram of genomic DNA from each sample was bisulfite-converted using EZ DNA Methylation-Gold kit (Zymo Research), according to the manufacturer's recommendations. Bisulfite-converted DNA was hybridized to the HumanMethylation27 BeadChip (Illumina inc.). Methylation levels of each CpG site were determined with fluorescent signals for methylated and unmethylated alleles. Methylated and unmethylated signals were used to compute a Beta value, which was a quantitative score of DNA methylation levels ranging from "0", for completely unmethylated, to "1", for completely methylated. On the HumanMethylation27 BeadChip, oligonucleotides for 27,578 CpG sites covering more than 14,000 genes are mounted, mostly selected from promoter regions. 26,956 (97.7%) out of the 27,578 CpG sites are set at promoters and 20,006 (72.5%) sites are set on CpG islands. CpG sites with ≥0.05 "Detection p value" (computed from the background based on negative controls) were eliminated from the data for further analysis, leaving 24,949 valid for use with the 16 samples tested.

Analysis of DNA methylation data

To analyze DNA methylation data, we used the following web tools: TIGR MeV [36] (http://www.tm4.org/mev.html) for hierarchical clustering heat map, NIA Array [37] (http://lgsun.grc.nia.nih.gov/ANOVA/) for hierarchical clustering that classify DNA methylation data by similarity and for principal component analysis (PCA) that finds major component in data variability, DAVID Bioinformatics Resources [38] (http://david.abcc.ncifcrf.gov/home.jsp), PANTHER Classification System [39] (http://www.pantherdb.org/), WebGestalt [40] (WEB-based GEne SeT AnaLysis Toolkit) (http://bioinfo.vanderbilt.edu/webgestalt/) based on based on KEGG (Kyoto Encyclopedia of Genes and Genomes) database [41] (http://www.genome.jp/kegg/) for gene ontology analysis, the GEO database (http://www.ncbi.nlm.nih.gov/geo/) for surveying gene expression in human iPS/ES cells (accession no. GSE9832 [16] and GSE12583 [17]), and the UCSC Genome Browser website [42] (http://genome.ucsc.edu/).

RT-PCR

RNA was extracted from cells using the RNeasy Plus Mini kit (Qiagen). An aliquot of total RNA was reverse transcribed using random hexamer primers. The cDNA template was amplified using specific primers for *SOX10*, *SOX15*, *PPP1R16B*, *SALL4*, *TDGF1*, *Sp100* and *GBP3*. Expression of glyceraldehyde-3-phosphate dehydrogenase (GAPDH) was used as a positive control. Primers used in this study are summarized in Table S6A.

Quantitative combined bisulfite restriction analysis (COBRA) and bisulfite sequencing

To confirm DNA methylation state, bisulfite PCR-mediated restriction mapping (known as the COBRA method) was performed. Sodium bisulfite treatment of genomic DNA was carried out as described above. PCR amplification was performed using IMMOLASE^{TM} DNA polymerase (Bioline Ltd; London, UK) and specific primers (Table S6B). After digestion with restriction enzymes, HpyCH4IV or Taq I, quantitative-COBRA coupled with the Shimadzu MCE®-202 MultiNA platform (Shimadzu, Japan) known as the Bio-COBRA method was carried out for quantitative DNA methylation level. Information of primers and restriction enzyme is summarized in Table S6B. To determine the methylation status of individual CpG in *SOX15*, *SALL4*, *Sp100* and *GBP3*, the PCR product was gel extracted and subcloned into pGEM T Easy vector (Promega, Madison, WI), and then sequenced. Methylation sites were visualized and quality control was carried out by the web-based tool, "QUMA" (http://quma.cdb.riken.jp/) [43].

Supporting Information

Table S1 Frequency of methylation states in each cell line.
Found at: doi:10.1371/journal.pone.0013017.s001 (0.04 MB PDF)

Table S2 A list of genes with SS-hyper-DMRs and SS-hypo-DMRs on KEGG Pathway.
Found at: doi:10.1371/journal.pone.0013017.s002 (0.05 MB PDF)

Table S3 (A) DNA methylation states of 23 genes (26 CpG sites) in Table 3, (B) DNA methylation states of 43 genes (50 CpG sites) in Table S4.
Found at: doi:10.1371/journal.pone.0013017.s003 (1.61 MB PDF)

Table S4 A list of 43 genes with SS-hyper-DMRs exhibiting 'low' expression in human iPS/ES cells.
Found at: doi:10.1371/journal.pone.0013017.s004 (0.07 MB PDF)

Table S5 (A) DNA methylation states of DNA methyltransferases, (B) Histone methylation states of DNA methyltransferases, (C) DNA methylation states of marker genes in human iPS/ES cells.
Found at: doi:10.1371/journal.pone.0013017.s005 (0.57 MB PDF)

Table S6 (A) primers used for RT-PCR, and (B) primers used for COBRA.
Found at: doi:10.1371/journal.pone.0013017.s006 (0.52 MB PDF)

Data set S1 A list of overlapped aberrant DMSs.
Found at: doi:10.1371/journal.pone.0013017.s007 (0.16 MB XLS)

Data set S2 A list of MRC-iPS specific aberrant DMSs.

Found at: doi:10.1371/journal.pone.0013017.s008 (0.13 MB XLS)

Data set S3 A list of AM-iPS specific aberrant DMSs.
Found at: doi:10.1371/journal.pone.0013017.s009 (0.25 MB XLS)

Data set S4 A list of SS-hyper-DMRs.
Found at: doi:10.1371/journal.pone.0013017.s010 (0.61 MB XLS)

Data set S5 A list of SS-hypo-DMRs.
Found at: doi:10.1371/journal.pone.0013017.s011 (0.10 MB XLS)

References

1. Thomson JA, Itskovitz-Eldor J, Shapiro SS, Waknitz MA, Swiergiel JJ, et al. (1998) Embryonic stem cell lines derived from human blastocysts. Science 282: 1145–1147.
2. Takahashi K, Tanabe K, Ohnuki M, Narita M, Ichisaka T, et al. (2007) Induction of pluripotent stem cells from adult human fibroblasts by defined factors. Cell 131: 861–872.
3. Huangfu D, Osafune K, Maehr R, Guo W, Eijkelenboom A, et al. (2008) Induction of pluripotent stem cells from primary human fibroblasts with only Oct4 and Sox2. Nat Biotechnol 26: 1269–1275.
4. Dimos JT, Rodolfa KT, Niakan KK, Weisenthal LM, Mitsumoto H, et al. (2008) Induced pluripotent stem cells generated from patients with ALS can be differentiated into motor neurons. Science 321: 1218–1221.
5. Woltjen K, Michael IP, Mohseni P, Desai R, Mileikovsky M, et al. (2009) piggyBac transposition reprograms fibroblasts to induced pluripotent stem cells. Nature 458: 766–770.
6. Li E (2002) Chromatin modification and epigenetic reprogramming in mammalian development. Nat Rev Genet 3: 662–673.
7. Reik W (2007) Stability and flexibility of epigenetic gene regulation in mammalian development. Nature 447: 425–432.
8. Hattori N, Nishino K, Ko YG, Ohgane J, Tanaka S, et al. (2004) Epigenetic control of mouse Oct-4 gene expression in embryonic stem cells and trophoblast stem cells. J Biol Chem 279: 17063–17069.
9. Nishino K, Hattori N, Tanaka S, Shiota K (2004) DNA methylation-mediated control of Sry gene expression in mouse gonadal development. J Biol Chem 279: 22306–22313.
10. Zingg JM, Pedraza-Alva G, Jost JP (1994) MyoD1 promoter autoregulation is mediated by two proximal E-boxes. Nucleic Acids Res 22: 2234–2241.
11. Tada M, Takahama Y, Abe K, Nakatsuji N, Tada T (2001) Nuclear reprogramming of somatic cells by in vitro hybridization with ES cells. Curr Biol 11: 1553–1558.
12. Nagata S, Toyoda M, Yamaguchi S, Hirano K, Makino H, et al. (2009) Efficient reprogramming of human and mouse primary extra-embryonic cells to pluripotent stem cells. Genes Cells 14: 1395–1404.
13. Makino H, Toyoda M, Matsumoto K, Saito H, Nishino K, et al. (2009) Mesenchymal to embryonic incomplete transition of human cells by chimeric OCT4/3 (POU5F1) with physiological co-activator EWS. Exp Cell Res 315: 2727–2740.
14. Cowan CA, Klimanskaya I, McMahon J, Atienza J, Witmyer J, et al. (2004) Derivation of embryonic stem-cell lines from human blastocysts. N Engl J Med 350: 1353–1356.
15. Brena RM, Auer H, Kornacker K, Plass C (2006) Quantification of DNA methylation in electrofluidics chips (Bio-COBRA). Nat Protoc 1: 52–58.
16. Park IH, Zhao R, West JA, Yabuuchi A, Huo H, et al. (2008) Reprogramming of human somatic cells to pluripotency with defined factors. Nature 451: 141–146.
17. Aasen T, Raya A, Barrero MJ, Garreta E, Consiglio A, et al. (2008) Efficient and rapid generation of induced pluripotent stem cells from human keratinocytes. Nat Biotechnol 26: 1276–1284.
18. Sperger JM, Chen X, Draper JS, Antosiewicz JE, Chon CH, et al. (2003) Gene expression patterns in human embryonic stem cells and human pluripotent germ cell tumors. Proc Natl Acad Sci U S A 100: 13350–13355.
19. Barski A, Cuddapah S, Cui K, Roh TY, Schones DE, et al. (2007) High-resolution profiling of histone methylations in the human genome. Cell 129: 823–837.
20. Mikkelsen TS, Ku M, Jaffe DB, Issac B, Lieberman E, et al. (2007) Genome-wide maps of chromatin state in pluripotent and lineage-committed cells. Nature 448: 553–560.
21. Bibikova M, Laurent LC, Ren B, Loring JF, Fan JB (2008) Unraveling epigenetic regulation in embryonic stem cells. Cell Stem Cell 2: 123–134.
22. Zhao XD, Han X, Chew JL, Liu J, Chiu KP, et al. (2007) Whole-genome mapping of histone H3 Lys4 and 27 trimethylations reveals distinct genomic compartments in human embryonic stem cells. Cell Stem Cell 1: 286–298.
23. Doi A, Park IH, Wen B, Murakami P, Aryee MJ, et al. (2009) Differential methylation of tissue- and cancer-specific CpG island shores distinguishes human induced pluripotent stem cells, embryonic stem cells and fibroblasts. Nat Genet 41: 1350–1353.
24. Fouse SD, Shen Y, Pellegrini M, Cole S, Meissner A, et al. (2008) Promoter CpG methylation contributes to ES cell gene regulation in parallel with Oct4/Nanog, PcG complex, and histone H3 K4/K27 trimethylation. Cell Stem Cell 2: 160–169.
25. Hong H, Takahashi K, Ichisaka T, Aoi T, Kanagawa O, et al. (2009) Suppression of induced pluripotent stem cell generation by the p53-p21 pathway. Nature 460: 1132–1135.
26. Kawamura T, Suzuki J, Wang YV, Menendez S, Morera LB, et al. (2009) Linking the p53 tumour suppressor pathway to somatic cell reprogramming. Nature 460: 1140–1144.
27. Utikal J, Polo JM, Stadtfeld M, Maherali N, Kulalert W, et al. (2009) Immortalization eliminates a roadblock during cellular reprogramming into iPS cells. Nature 460: 1145–1148.
28. Marion RM, Strati K, Li H, Murga M, Blanco R, et al. (2009) A p53-mediated DNA damage response limits reprogramming to ensure iPS cell genomic integrity. Nature 460: 1149–1153.
29. Li H, Collado M, Villasante A, Strati K, Ortega S, et al. (2009) The Ink4/Arf locus is a barrier for iPS cell reprogramming. Nature 460: 1136–1139.
30. Maherali N, Hochedlinger K (2009) Tgfbeta Signal Inhibition Cooperates in the Induction of iPSCs and Replaces Sox2 and cMyc. Curr Biol 18: 1718–1723.
31. Bibikova M, Chudin E, Wu B, Zhou L, Garcia EW, et al. (2006) Human embryonic stem cells have a unique epigenetic signature. Genome Res 16: 1075–1083.
32. Deng J, Shoemaker R, Xie B, Gore A, LeProust EM, et al. (2009) Targeted bisulfite sequencing reveals changes in DNA methylation associated with nuclear reprogramming. Nat Biotechnol 27: 353–360.
33. Mori T, Kiyono T, Imabayashi H, Takeda Y, Tsuchiya K, et al. (2005) Combination of hTERT and bmi-1, E6, or E7 induces prolongation of the life span of bone marrow stromal cells from an elderly donor without affecting their neurogenic potential. Mol Cell Biol 25: 5183–5195.
34. Cui CH, Uyama T, Miyado K, Terai M, Kyo S, et al. (2007) Menstrual blood-derived cells confer human dystrophin expression in the murine model of Duchenne muscular dystrophy via cell fusion and myogenic transdifferentiation. Mol Biol Cell 18: 1586–1594.
35. Jacobs JP, Jones CM, Baille JP (1970) Characteristics of a human diploid cell designated MRC-5. Nature 227: 168–170.
36. Saeed AI, Sharov V, White J, Li J, Liang W, et al. (2003) TM4: a free, open-source system for microarray data management and analysis. Biotechniques 34: 374–378.
37. Sharov AA, Dudekula DB, Ko MS (2005) A web-based tool for principal component and significance analysis of microarray data. Bioinformatics 21: 2548–2549.
38. Huang da W, Sherman BT, Lempicki RA (2009) Systematic and integrative analysis of large gene lists using DAVID bioinformatics resources. Nat Protoc 4: 44–57.
39. Mi H, Lazareva-Ulitsky B, Loo R, Kejariwal A, Vandergriff J, et al. (2005) The PANTHER database of protein families, subfamilies, functions and pathways. Nucleic Acids Res 33: D284–288.
40. Zhang B, Kirov S, Snoddy J (2005) WebGestalt: an integrated system for exploring gene sets in various biological contexts. Nucleic Acids Res 33: W741–748.
41. Kanehisa M, Araki M, Goto S, Hattori M, Hirakawa M, et al. (2008) KEGG for linking genomes to life and the environment. Nucleic Acids Res 36: D480–484.
42. Kent WJ, Sugnet CW, Furey TS, Roskin KM, Pringle TH, et al. (2002) The human genome browser at UCSC. Genome Res 12: 996–1006.
43. Kumaki Y, Oda M, Okano M (2008) QUMA: quantification tool for methylation analysis. Nucleic Acids Res 36: W170–175.

Acknowledgments

We would like to express our sincere thanks to Drs. M. Yamada and K Miyado for discussion and critical reading of the manuscript, to Drs. C. Cowan and T. Tenzan for HUES cell lines, to Dr. D. Kami for establishing the PAE551 cell line, to K. Miyamoto for bisulfite sequencing, to Drs. K. Hata and K. Nakabayashi for COBRA.

Author Contributions

Conceived and designed the experiments: KN AU. Performed the experiments: KN MT MYI. Analyzed the data: KN YT. Contributed reagents/materials/analysis tools: KN MT MYI HM YF EC YM HO NK HA. Wrote the paper: KN AU.

Biomed Microdevices (2010) 12:1097–1105
DOI 10.1007/s10544-010-9464-8

Enhanced effects of secreted soluble factor preserve better pluripotent state of embryonic stem cell culture in a membrane-based compartmentalized micro-bioreactor

Mohammad Mahfuz Chowdhury · Takeshi Katsuda · Kevin Montagne · Hiroshi Kimura · Nobuhiko Kojima · Hidenori Akutsu · Takahiro Ochiya · Teruo Fujii · Yasuyuki Sakai

Published online: 1 September 2010

Abstract Pluripotent stem cells are under the influence of soluble factors in a diffusion dominant *in vivo* microenvironment. In order to investigate the effects of secreted soluble factors on embryonic stem cell (ESC) behavior in a diffusion dominant microenvironment, we cultured mouse ESCs (mESCs) in a membrane-based two-chambered micro-bioreactor (MB). To avoid disturbing the cellular environment in the top chamber of the MB, only the culture medium of the bottom chamber was exchanged. Cell growth in the MB after 5 days of culture was similar to that in conventional 6-well plate (6-WP) and membrane-based Transwell insert (TW) cultures, indicating adequate nutrient supply in the MB. However, the cells retained higher expression of pluripotency markers (Oct4, Sox2 and Rex1) and secreted soluble factors (FGF4 and BMP4) in the MB. Inhibition of FGF4 activity in the MB and TW resulted in a similar cellular response. However, in contrast to the TW, inhibition of BMP4 activity revealed that autocrine action of the upregulated BMP4, which acted cooperatively with leukemia inhibitory factor (LIF), upregulated the pluripotency markers expression in the MB culture. We propose that BMP4 accumulated in the diffusion dominant microenvironment of the MB upregulated its own expression by a positive feedback mechanism—in contrast to the macro-scale culture systems—thereby enhancing the pluripotency of mESCs. The micro-scale culture platform developed in this study enables the investigation of the effects of soluble factors on ESCs in a diffusion dominant microenvironment, and is expected to be used to modulate the ESC fate choices.

Keywords Embryonic stem cell · Soluble factors · Diffusion · Microenvironment · Micro-bioreactor

M. M. Chowdhury (✉) · T. Katsuda · K. Montagne · H. Kimura · N. Kojima · T. Fujii · Y. Sakai
Institute of Industrial Science,
The University of Tokyo,
Tokyo, Japan
e-mail: mahfuz@iis.u-tokyo.ac.jp

K. Montagne · T. Fujii · Y. Sakai
LIMMS/CNRS-IIS, The University of Tokyo,
Tokyo, Japan

H. Akutsu
Department of Reproductive Biology,
National Research Institute for Child Health and Development,
Tokyo, Japan

T. Ochiya
Section for Studies on Metastasis,
National Cancer Center Research Institute,
Tokyo, Japan

1 Introduction

The autocrine and paracrine actions of soluble factors have an important role in directing pluripotent stem cell fate choices *in vivo* (Gadue et al. 2005; Loebel et al. 2003). Pluripotent stem cells and their progenies remain in a diffusion dominant microenvironment enclosed by the trophectoderm and extra-embryonic part until an appreciable amount of mass flow by convection occurs after the onset of blood circulation (Nagy et al. 2003). At the initial stage of embryo development, the fate of pluripotent cells is influenced by the adequate signaling

of soluble factors in the microenvironment. *In vitro*, ESC fate is also modulated by soluble factors (Kunath et al. 2007; Ying et al. 2003a). Although exogenous soluble factors can be added to the *in vitro* culture systems to control ESC fate, it is necessary to consider the influence of endogenous soluble factors which are secreted by the cells (Wiles and Proetzel 2006). This is highlighted by the fact that the addition of exogenous soluble factors has little influence on the initial differentiation of embryoid bodies (EBs) but influences the successive maturation of differentiated progenies towards the matured cell types (Ogawa et al. 2005; Wiles and Proetzel 2006). Furthermore, neuronal stem cells can be derived efficiently from mouse ESCs (mESCs) without the addition of exogenous factors (Ying et al. 2003b). Therefore, a culture system which mimics the diffusion dominant nature of the *in vivo* microenvironment is of great importance in order to improve our understanding of stem cell biology and control the stem cell fate decision (Loebel et al. 2003; Murry and Keller 2008).

Microfluidic technology provides advanced tools to develop micro-scale culture systems in an *in vivo* relevant dimension as well as to control mass transfer modes in the cellular microenvironment (Meyvantsson and Beebe 2008). Various micro-scale culture systems have been developed for ESC culture, but little is known about the effects of secreted soluble factors in these systems. Moreover, before proceeding to the differentiation of ESCs, it is necessary to characterize the differences between the micro and macro-scale cultures, namely regarding the effects of cell secreted soluble factors on ESC behavior. Human ESCs (hESCs) cells were cultured in straight micro-channels in static (Abhyankar et al. 2003) and semi-static (Korin et al. 2009) conditions. Although these cultures facilitated the accumulation of soluble factors around the cells owing to the diffusion dominant nature of static micro-scale culture, their effects on the cells were not investigated. Furthermore, the environment changed abruptly because of the daily replacement of the total culture medium. In micro-fabricated wells, hESCs were found to remain undifferentiated for more than two weeks (Mohr et al. 2006). The reason for that was not identified, but most likely resulted from soluble factors, cell-cell contacts and the extra-cellular matrix (ECM) produced by the cells. Some studies focused on controlling ESC microenvironment using perfusion-based systems (Figallo et al. 2007; Kim et al. 2006). In one of those studies, mESCs were cultured in microfluidic arrays at different flow rates, and the cell colonies showed flow-dependent size variations (Kim et al. 2006). This was attributed to the amount of nutrient delivery as well as the removal of waste and secreted factors. Although perfusion is a way to supply enough nutrients to cells for long-term culture and control the cellular microenvironment by removal of the secreted soluble factors, it disturbs the cellular diffusion-based microenvironment (Walker et al. 2004).

In this context, we developed a membrane-based two-chambered micro-bioreactor (designated as MB hereafter) and culture conditions for ESCs to investigate the influence of secreted soluble factors on cells by mimicking the diffusion-dominant *in vivo* microenvironment. The culture medium of the top chamber was not replaced during the culture period to avoid disturbance in the cellular microenvironment. In contrast, the culture medium of the bottom chamber was exchanged daily to maintain a sufficient nutrient supply. We cultured mESCs for five days in leukemia inhibitory factor (LIF) supplemented culture medium to study the effects of soluble factors on cellular behavior, such as cell-cell interactions, cell proliferation and differentiation, in which the influence of secreted soluble factors is important (Yu et al. 2005). In the LIF supplemented medium, BMP4 synergistically interacts with LIF to preserve the mESC pluripotency by resisting the differentiation inducing action of FGF4 (Ying et al. 2008c). Therefore, the cell states in the MB, membrane-based macro-scale Transwell Insert (TW) and conventional 6-well plate (6-WP) cultures were compared by the expression of pluripotency markers (Oct4, Sox2, Rex1 and Nanog) and cell secreted soluble factors (FGF4 and BMP4). In addition, we performed cell culture experiments by inhibiting signaling components of FGF4 and BMP4 in the MB and TW. Then, the gene expressions of inhibited and non-inhibited cultures were compared to discern the effects of soluble factors in the micro and macro-scale culture systems.

2 Materials and methods

2.1 Design of the MB

Figure 1 shows the design details of the MB. The reactor had two round chambers (top and bottom) with an area of 2.27 cm^2. They were kept separated by a porous membrane. Each of the chambers' height and volume were 500 μm and 114 μL, respectively. The chambers contained 13 pillars (1 mm in diameter) that kept the membrane horizontal, and enabled a more homogeneous cell seeding on the membrane. Cells were cultured on the top face of the membrane. To avoid culture area other than the membrane, two feeding holes in the top chamber were drilled at the chamber perimeter. On the other hand, feeding holes in the bottom chamber were made approximately 0.7 cm away from the chamber perimeter to get clearance from the membrane perimeter.

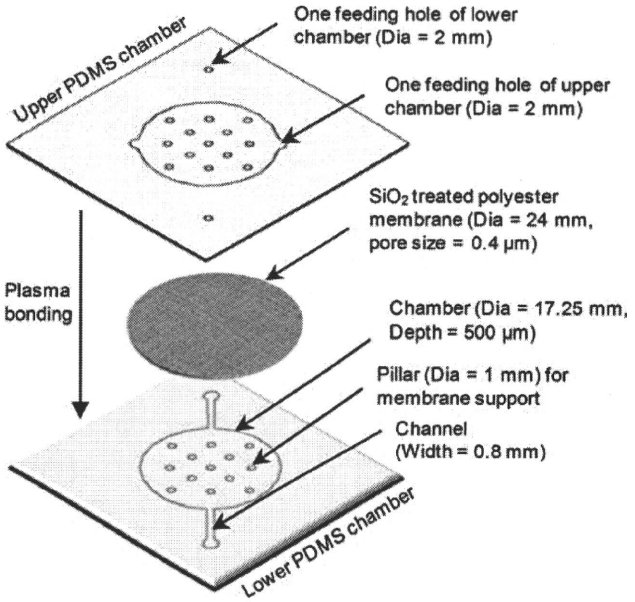

Fig. 1 Details of the PDMS chambers and membrane used to fabricate the MB. The membrane is sandwiched between the two PDMS chambers using the common O_2 plasma method. Both top and bottom PDMS chambers have two feeding holes to inject cells and exchange culture medium. Cells are cultured only on the top face of membrane

2.2 Fabrication of the MB

Details of the MB fabrication method are presented elsewhere (Kimura et al. 2008). Briefly, negative photoresist SU-8 2100 (Microchem Co.) was used to create the mold masters with the desired pattern. Then PDMS polymer (Silpot 184; Dow Corning Corp.) was mixed with its curing agent at a 10:1 ratio, poured over the mold masters, cured for 2 h at 75°C and peeled off thereafter.

The polyester membranes (pore size 0.4 μm, thickness 10 μm) were removed from Transwell Inserts 3450 (Corning Inc.). To bond the membrane with the PDMS layers, both sides of the membrane were coated with a thin layer of SiO_2 by sputtering for 20 s at 150 W and 0.5 Pa. The membrane was sandwiched between the two PDMS chambers following O_2 plasma treatment. Flow chips were then attached to the silicon tubing for connecting syringes; medium and reagents were manually introduced using those syringes.

2.3 Pre-treatment of experimental group (6-WP, TW and MB)

Because SiO_2 was used to coat the polyester membrane incorporated in the MB, the top side of the TW membrane was also coated with SiO_2 by sputtering. The TW and MB were then sterilized for 2 h under UV light. A 0.2% w/v gelatin solution was applied to cover the surface of the 6-WP and the membrane surfaces of the TW and MB, which was followed by 6 h of incubation. Culture medium for the experimental group was added to these culture systems for pre-incubation before seeding mESCs.

2.4 Routine cell culture

mESCs were routinely cultured in 60 mm gelatin coated dishes (Iwaki). Cell inoculation density was 2×10^4 cells/cm^2, and the cells were passaged every other day. Culture medium composition for routine culture was high glucose DMEM (DMEM; Gibco) containing 20% ESC qualified Fetal Bovine Serum (FBS; Gibco), 1000 U/ml ESGRO-LIF (Chemicon), 1% MEM non-essential amino acids (Gibco), 2 mM GlutaMax-I (Gibco), 100 U/ml penicillin, 100 U/ml streptomycin (Gibco) and 0.1 mM 2-mercaptoethanol (Gibco). The cells were maintained in a 37°C humidified environment containing 5% CO_2.

2.5 Cell culture in the experimental group

mESCs in the experimental group were cultured using the same medium as for routine culture except that DMEM and FBS were replaced with Knockout DMEM (Gibco) and 15% Knockout Serum (KSR; Gibco), respectively. KSR was used because it contains fewer extrinsic proteins. For the experimental group, cell inoculation density was 2×10^4 cells/cm^2. Cell culture in the experimental group was continued for 5 days. Culture medium of the 6-WP, the lower chambers of the TW and MB were changed daily. The upper chamber culture medium of the TW and MB were not changed. Morphological examination of the cells under microscope was performed daily. For inhibition experiments, Fibroblast Growth Factor Receptor (FGFR) antagonist SU5402 (Mohammadi 1997) (Calbiochem) at 10 μM and BMP4 antagonist Noggin (Smith and Harland 1992) (R&D Systems) at 100 ng/ml were added to the culture medium.

2.6 Glucose concentration measurement

Culture medium from the 6-WP, the lower chamber of the TW and MB were collected every day during the 5-day culture. On the 5th day, the culture medium from the upper chambers of the TW and MB were also collected. Glucose concentrations were measured with a glucose analyzer (GA05, A&T Corp., Japan).

2.7 Cell collection and qPCR analysis

Isolation of total mRNA was performed using Trizol Reagent (Invitrogen). In all culture systems, cells were dissociated using Trypsin (Gibco), counted and then lysed with Trizol. First-Strand cDNA Synthesis Kit (GE

Healthcare) was used to synthesize cDNA from the total mRNA. PCR reactions were carried out with a 7500 Real-Time PCR System (Applied Biosystems) using Quantitect SYBR Green PCR Kit (Qiagen). All steps were performed according to the manufacturers' instructions. Primers for cDNA amplification are listed in Table 1. qPCR were performed at least in duplicate. Raw data of PCR product amplification curves was analyzed using LinRegPCR v11.4 software (Ruijter et al. 2009) to determine the threshold cycles used in the $\Delta\Delta C_T$ method for relative quantification of gene expression. Geometric mean of the threshold cycles of reference genes GAPDH and β-Actin was used to normalize the target gene expressions. mESC culture at day 3 in the 6-WP was used as calibrator.

2.8 Statistical analysis

Student's *t*-test for comparing two groups and one way ANOVA with Tukey's post test for comparing more than two groups were performed for statistical evaluation using the demo version of GraphPad software (GraphPad Software, Inc.). Differences with a $P<0.05$ (*), $P<0.01$ (**), or $P<0.001$ (***) were considered to be statistically significant. All data are presented as the mean ± SEM.

3 Results

3.1 Effect of SiO_2 coating of the membranes on ESC behavior

SiO_2 coating on the membrane was necessary to bond it strongly with the PDMS layers, thereby preventing culture medium leakage in the MB. The coating did not affect permeability of the membranes as the measured glucose permeability of coated and non-coated membranes was the same (3×10^{-12} m^2s^{-1}). To examine whether the coating had any effect on cell behavior, we performed mESC culture on SiO_2-coated and non-coated membranes of the TW. Spread colonies of mESCs were observed on SiO_2-coated membranes (Fig. 2(a)), whereas these colonies remained spherical on the non-coated membranes (Fig. 2(b)). Cells attached weakly on the membranes without SiO_2 coating as the PBS wash during cell harvesting caused some cell loss. Consequently, the PBS wash was omitted for the non-coated membranes. However, no difference in cell growth was observed between SiO_2-coated and non-coated samples (fold changes in cell number relative to the seeded cells were 35.25±2.58 and 36.72±3.51, respectively). Furthermore, both of the cultures showed similar gene expression profile ($P>0.05$) (Fig. 3). Therefore, SiO_2 coating on the membrane was used for all the experiments.

3.2 Cell culture condition in the 6-WP, TW and MB

To keep the cellular microenvironment in the upper chamber of the MB and TW minimally disturbed, we only changed the culture medium of the lower chambers. Despite this, nutrients in these culture systems were sufficient as the glucose concentration throughout the 5 days of culture remained over half of the glucose concentration in fresh culture medium (0.02 M). Furthermore, no significant cell death was observed as assessed by the Trypan blue dye-exclusion test (data not shown) on day 5. Cell growth in all culture systems was similar ($P>0.05$) (Fig. 4). mESC culture in the TW and MB could be continued for more

Table 1 Genes and primers used in qPCR analyses

Genes	Description	Primer	Sequence (5′-3′)
GAPDH	Housekeeping gene	Forward	CAGAACATCATCCCTGCATC
		Reverse	CTGCTTCACCACCTTCTTGA
β-Actin	Housekeeping gene	Forward	TCACCCACACTGTGCCCATCTACGA
		Reverse	CAGCGGAACCGCTCATTGCCAATGG
Oct4	Pluripotency marker	Forward	AGAACCTTCAGGAGATATGC
		Reverse	TCTTCTCGTTGGGAATACTC
Sox2	Pluripotency marker	Forward	ACAAGGAAGGAGTTTATTCG
		Reverse	TTACCAACGATATCAACCTG
Rex1	Pluripotency marker	Forward	ACACAGAAGAAAGCAGGAT
		Reverse	GAACAATGCCTATGACTCAC
Nanog	Pluripotency marker	Forward	TGATTCTTCTACCAGTCCC
		Reverse	GGTCTTAACCTGCTTATAGC
FGF4	Cells' self-secreted soluble factor	Forward	TCGGTGTGCCTTTCTTTACC
		Reverse	ACCTTCATGGTAGGCGACAC
BMP4	Cells' self-secreted soluble factor	Forward	CCATCACGAAGAACATCTG
		Reverse	AATGTTTATACGGTGGAAGC

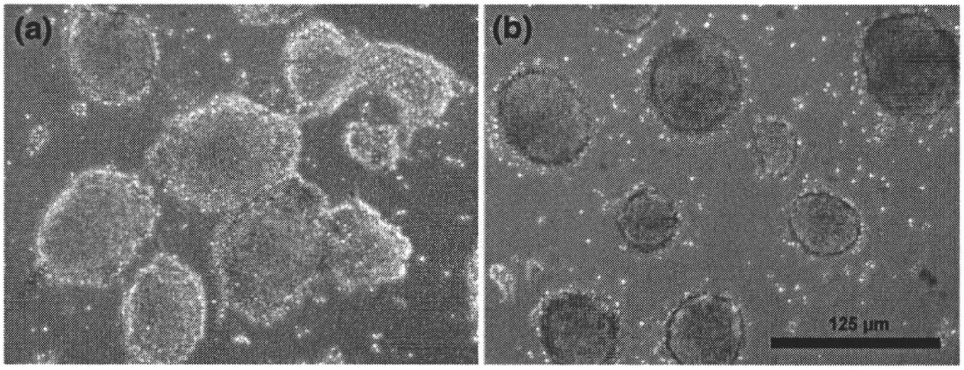

Fig. 2 mESC culture on day 5 on SiO_2-coated (**a**) or non-coated (**b**) polyester membranes of the TW. Cell colonies on the SiO_2-coated membrane are spread, whereas colonies on the non-coated membrane are round. Scale bar represents 125 μm

than 5 days, whereas cells began to die in the 6-WP after that period owing to nutrition depletion.

mESC colonies were extensively merged in the 6-WP (Fig. 5(a)) but they remained mostly as separated colonies in the TW and MB on day 5 (Fig. 5(b) and (c), respectively). Many differentiated cells showing a different morphology from usual mESCs were observed in the vicinity of cell colonies in the 6-WP and TW cultures (Fig. 5(d) and (e), respectively). In contrast, a few differentiated cells and smooth-bordered mESC colonies were observed in the MB (Fig. 5(f)), thereby indicating homogenous nature of the colonies.

3.3 Comparison of gene expression profiles among culture systems

In the MB culture, significantly higher expression levels of Oct4, Sox2 and Rex1 were observed compared to the 6-WP (Fig. 6). In addition, Sox2 and Rex1 expression in the MB were considerably higher than in the TW culture. These results showed that mESC pluripotency in the MB culture was higher than that in the macro-scale culture systems (6-WP and TW). Furthermore, both FGF4 and BMP4 were highly expressed in the MB culture compared to the TW (Fig. 6). However, only BMP4 expression in the MB was observed to be higher than in the 6-WP. Only Rex1 expression was different between the TW and 6-WP (Fig. 6).

3.4 Effects of soluble factors

To investigate whether dissimilarity in the activities of FGF4 and BMP4 between the MB and TW was responsible for the observed differences in the pluripotency markers expression (Sox2 and Rex1; Fig. 6), we performed inhibition experiments of FGF4 and BMP4 activities in the MB and TW cultures. FGF4 activity was inhibited using the small molecule SU5402, an antagonist of FGFR. This resulted in significantly increased expression of Nanog in the MB as well as TW cultures, but the other three pluripotency markers remained essentially unchanged (Fig. 7(a)). Expression of FGF4 increased, whereas that of BMP4 decreased in both MB and TW (Fig. 7(a)). We therefore concluded that the differentiation inducing activity of FGF4 suppressed Nanog expression, but did not affect the expression of Sox2 and Rex1 in the TW or MB. As a result, FGF4 cannot be

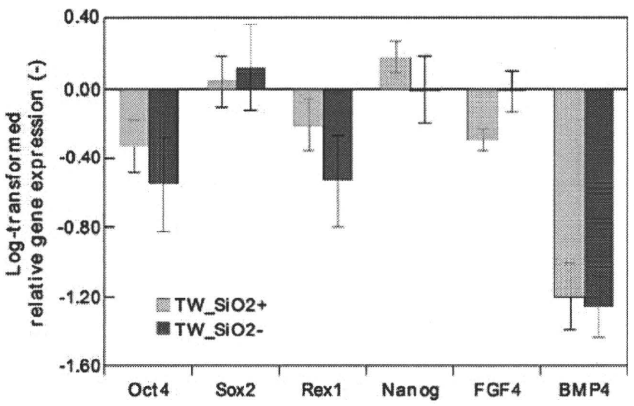

Fig. 3 Relative gene expression (Log_2-transformed) of mESCs cultured for 5 days on SiO_2-coated (TW_SiO2+) or non-coated (TW_SiO2−) membrane of the TW. Both cultures show similar gene expression profiles ($P>0.05$). Zero value represents the gene expression of mESC cultured in 6-WPs for 3 days. Columns and error bars represent mean ± SEM of three independent experiments

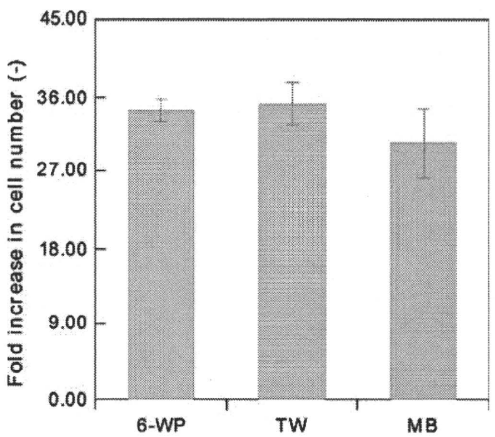

Fig. 4 Fold increase in cell number relative to the seeded cell number after 5 days of mESC culture in the 6-WP, TW and MB. Cell growths are similar in all culture systems ($P>0.05$). Columns and error bars represent mean ± SEM of four independent experiments

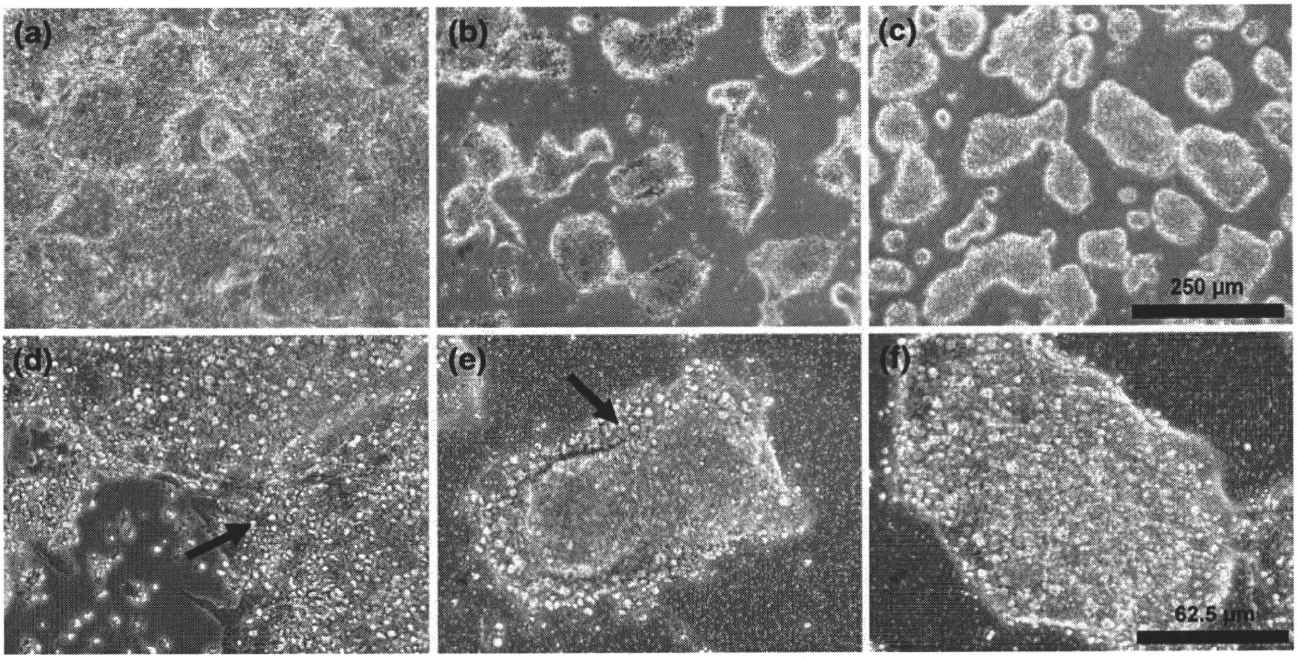

Fig. 5 mESC culture on day 5 in the 6-WP (**a**, **d**), TW (**b**, **e**) and MB (**c**, **f**). Arrows in the higher magnification images (**d**, **e**) indicate differentiated cells with a different morphology from the tightly packed colony type morphology of mESCs. Scale bars represents 250 μm (**a**, **b** and **c**), and 62.5 μm (**d**, **e** and **f**)

accounted for the differences in Sox2 and Rex1 expressions between the MB and TW cultures.

We then inhibited BMP4 activity using its antagonist Noggin. Expression of the pluripotency markers Sox2 and Rex1 decreased by the Noggin treatment in the MB, but they remained unchanged in the TW (Fig. 7(b)). In addition, both in the MB and TW culture, FGF4 and BMP4 expression remained unchanged by the same treatment. Sox2 and Rex1, which were upregulated more significantly in the MB as compared to the 6-WP and TW cultures (Fig. 6), decreased significantly by the Noggin treatment (Fig. 7(b)). Therefore, we can conclude that the activity of upregulated BMP4 (Fig. 6) is responsible for the better preservation of the mESC pluripotency in the MB.

4 Discussion

In this study, we developed a micro-scale culture system in which ESCs can be cultured in a diffusion dominant

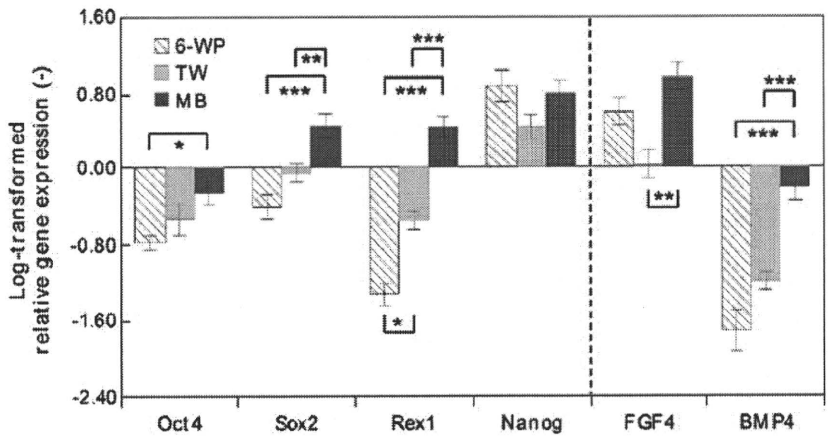

Fig. 6 Comparison of the gene expression profiles (Log_2-transformed) of mESCs cultured for 5 days in the 6-WP, TW and MB. Pluripotency markers (Oct4, Sox2 and Rex1) and soluble factors (FGF4 and BMP4) expression are upregulated in the MB. Zero represents gene expression of mESCs cultured in the 6-WP for 3 days. Columns and error bars represent mean ± SEM of six independent experiments. Statistical significance of the compared pairs are shown using the symbols *, ** and ***, representing *P*-values below 0.05, 0.01 and 0.001, respectively

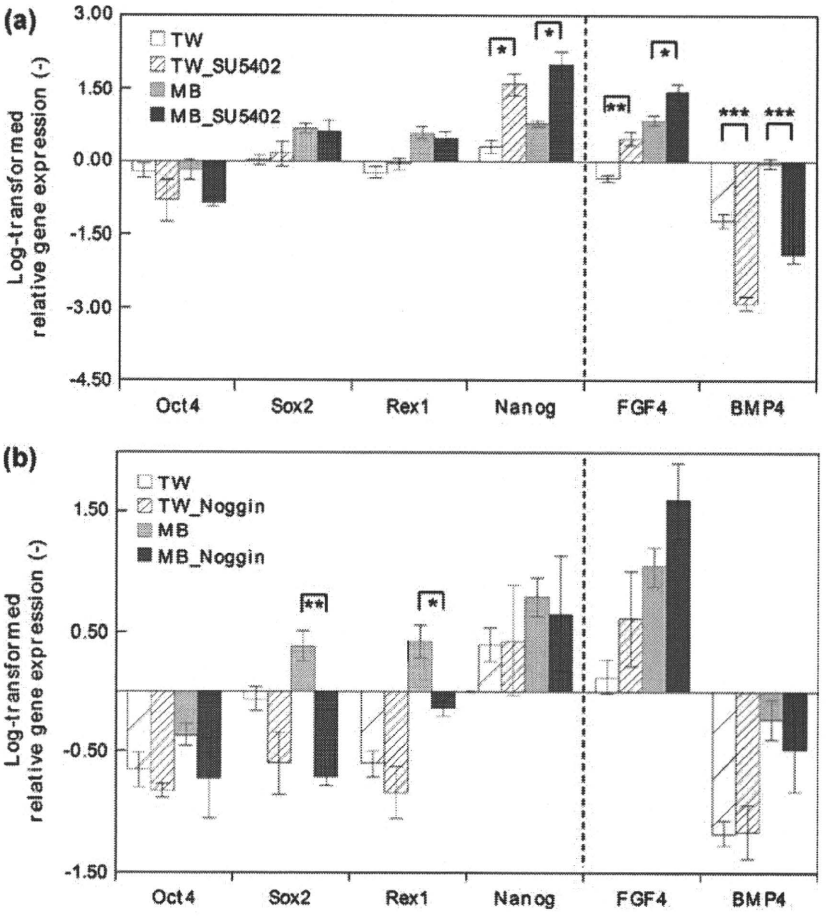

Fig. 7 Gene expression profiles (Log_2-transformed) of mESCs cultured for 5 days in the TW and MB, (**a**) with (TW_SU5402 and MB_SU5402) or without (TW and MB) inhibition of FGF4 signaling by SU5402; (**b**) with (TW_Noggin and MB_Noggin) or without (TW and MB) the BMP4 antagonist Noggin. Nanog expression both in the TW and MB increases following the SU5402 treatment. Sox2 and Rex1 expression decrease only in the MB following the Noggin treatment. Zero represents gene expression of mESCs cultured in 6-WP for 3 days. Columns and error bars represent mean ± SEM of four and three independent experiments for (a) and (b), respectively. Statistical significance of the compared pairs (TW against TW_SU5402; MB against MB_SU5402; TW against TW_Noggin; MB against MB_Noggin) are shown using symbols *, ** and ***, representing *P*-values below 0.05, 0.01 and 0.001, respectively

microenvironment without any limitation of nutrient supply for a long period of time. We observed better preservation of the mESC pluripotency in the micro-bioreactor than in the conventional macro-scale 6-WP and TW culture systems. We also demonstrated that autocrine effects of the up-regulated BMP4 cooperated with LIF to preserve the high pluripotency in the MB. Furthermore, the influence of FGF4 was similar in the TW and MB, whereas the influence of BMP4 was observed only in the MB.

A transcription network of Oct4, Sox2, Rex1 and Nanog maintains the pluripotency and proliferation of mESCs by suppressing the gene expression associated with differentiation (Masui et al. 2008; Niwa 2007). Usually, even in undifferentiated culture of mESCs in the presence of LIF, a proportion of the cells can undergo spontaneous differentiation (Smith 2001) which is associated with the decreased expression of those genes. Generally, overgrown differentiating mESC colonies have rough borders compared to the normal colonies. In the MB, mESC colonies were smooth-bordered, had few differentiated cells (Fig. 5(c) and (f)) and retained higher expression of the pluripotency markers (Fig. 6). These results indicated spontaneous differentiation of ESCs occurred less in the MB. Among the pluripotency markers, Sox2 and Rex1 showed prominently higher expression in the MB as compared to the WP and TW (Fig. 6). In fact, downregulation of Sox2 and Rex1 expression has a stronger correlation with loss of pluripotency of mESCs than the downregulation of Oct4 and Nanog expression (Palmqvist et al. 2005).

mESCs produce FGF4 extensively (Niwa et al. 2000) and BMP4 moderately (Johansson and Wiles 1995). FGF4 induces mESCs to differentiate (associated with the decreased expression of pluripotency markers of mESCs), which is counteracted by LIF and BMP4, as shown in Fig. 8 (Ying et al. 2008). In this study, although FGF4 was upregulated, high expression of BMP4 cooperated with LIF to preserve a high expression of pluripotency markers in the MB (Figs. 6, 7(b) and 8). In contrast, downregulated BMP4 in the TW had no observable effect on mESC pluripotecny markers, thereby maintaining a low level of pluripotency markers expression (Figs. 7(b) and 8). Notably, BMP4 expression was significantly upregulated only in the MB culture compared to the 6-WP and TW cultures (Fig. 6). Enclosed micro-scale environment might have facilitated the upregulation of BMP4 in the MB. Because the cell growth behaviors in these cultures were the same (Fig. 4), amount of secreted factors in the culture environment would be approximately the same. However, in the MB,

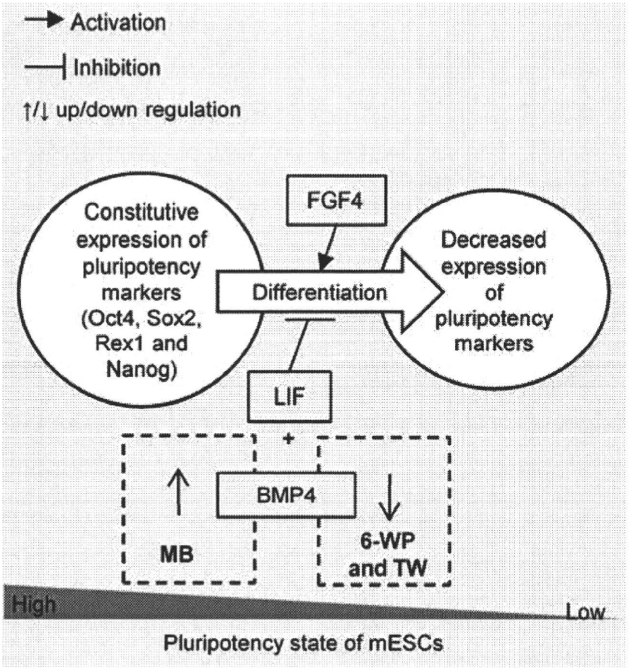

Fig. 8 A schematic diagram of the influence of soluble factors on the pluripotency markers in the embryonic stem cell culture environment. LIF and BMP4 cooperate to resist FGF4-induced differentiation. Effects of BMP4 on the pluripotency state of mESCs in the micro (MB) and macro-scale (TW) culture systems are also depicted

the culture volume was small (114 μL compared to the cell compartment volumes of 1.5 mL and 2 mL in the TW and 6-WP, respectively), and mass transfer was diffusion dominant due to small dimensions as well as the absence of a free interface between the culture medium and air (Yu et al. 2005). On the other hand, surface tension differences at the interface cause rapid convection in the macro-scale culture systems, and that creates a homogenous distribution of secreted soluble factors over the entire culture volume (Yu et al. 2005). Therefore, secreted soluble factors were accumulated and reached higher concentrations in the MB than in the 6-WP and TW. Moreover, they were presumably retained around the cell colonies at high concentrations for a longer time period in the MB owing to the diffusion dominant mass transfer. BMP4 can induce its own expression by a positive feedback mechanism (Vainio et al. 1993). Furthermore, owing to the relatively short half-life of BMP4, it is necessary to retain BMP4 near the cell for its activity (Miljkovic et al. 2008). Therefore, the higher exposure of cells to BMP4 in the MB culture than in the macro-scale cultures (the 6-WP and TW) may facilitate the feedback mechanism. This explains the observed upregulation and downregulation of BMP4 expression in the MB and macro-scale cultures, respectively (Fig. 6).

In spite of FGF4 accumulation, cells in the MB displayed a similar response in gene expression to that observed in the TW following FGF4 inhibition (Fig. 7(a)). However, inhibition of BMP4 activities resulted in significantly different effects in the MB and TW (Fig. 7(b)). Molecular diffusivities (inversely proportional to the cube root of molecular weight, MW) primarily determine the retention behavior of the soluble factors around the cells (Yu et al. 2005). FGF4 has a lower MW (22 kDa) than BMP4 (47 kDa), and may have diffused more quickly out of the cellular milieu. Therefore, it was unable to exert any influence on the cells as BMP4 did in the MB. In addition, extensively secreted FGF4 could have reached the threshold level of its activity equally in the MB and TW. These could be the plausible reason for the similar response observed in the TW and MB.

The average concentrations (total number of molecules divided by volume) of FGF4 and BMP4 in the MB might be the highest among the culture systems owing to the accumulation of these factors in the smallest volume. However, the cellular response to a soluble factor depends on the concentration level of the factor in the vicinity of the cell (local concentration). Both the average and local concentrations are influenced by various parameters of a soluble factor such as secretion, consumption, sequestration and release form the ECM. However, convection and diffusion only influence the local concentration. Owing to the diffusion dominant mass transfer in the MB, a soluble factor could be retained around the cells over time to reach a high concentration—all other parameters being the same in all culture systems. Therefore, in the MB, we could realize the combined effect of accumulation in a small volume and diffusion dominant mass transfer. However, we could not distinguish explicitly which concentration (average or local) reached the threshold level to impart a cellular response. To make the distinction, further investigation (experiments coupled with mathematical simulation) is necessary by taking the various parameters of a soluble factor into account along with diffusion and convection. This study, which characterizes the effects of soluble factors on ESC culture in the MB, provides a basis for the investigation.

mESCs secret FGF5, Nodal and BMP2 at low variable levels besides FGF4 and BMP4 (Wiles and Proetzel 2006). This micro-bioreactor and culture condition will be useful to study their effects in a diffusion dominant cellular environment, and will contribute to the understanding of ESC biology. The heterogeneity of ESCs during differentiation is one obstacle in obtaining lineage-specific cells useful for cell-based transplantation therapies (Singh and Terada 2007). Our micro-bioreactor can be used for obtaining relatively homogenous ESCs. In the absence of LIF, both FGF4 and BMP4 promote the differentiation of ESCs (Ying et al. 2003a). Therefore, the activity of soluble factors observed in the MB will provide an enhanced signaling microenvironment for controlling ESC differenti-

ation process in a monolayer format such as for neuronal (Ying et al. 2003b) or hepatocyte (Teratani et al. 2005) differentiation. By keeping the cellular environment in the upper chamber minimally disturbed, it is also possible to provide other soluble factors or inhibitors through the lower chamber to gain more precise control of the differentiation process.

5 Conclusions

In this study, we developed a membrane-based two-chambered micro-bioreactor for mESC culture to mimic the diffusion dominant mass transfer environment observed *in vivo*. The influence of soluble factors on cells in the micro-bioreator was compared with a macro-scale culture system. We observed enhanced retention of the pluripotent phenotype of mESCs in the micro-bioreactor owing to the enhanced effect of a soluble factor in a diffusion dominant microenvironment. A similar effect of the soluble factor was not observed in the macro-scale membrane-based Transwell insert culture system, in which soluble factors dissipated away from cell surrounding through inherent convection. This micro-bioreactor offers a suitable platform not only to understand the influence of secreted soluble factors on stem cell biology, but also to address an enhanced signaling environment to direct the ESC fate.

Acknowledgements M. M. Chowdhury was supported by Monbukagakusho scholarship from the Japan Ministry of Education, Culture, Sports, Science and Technology (MEXT). This research was supported in part by CREST from Japan Science and Technology Agency and GMSI (Global Center of Excellence for Mechanical Systems Innovation), The University of Tokyo. We would like to thank Dr. Masaki Nishikawa and Dr. Morgan Hamon for their useful suggestions regarding various technical aspects related to this study.

References

V.V. Abhyankar, G.N. Bittner, T.J. Kamp, D.J. Beebe, in 7th International Conference on Miniaturized Chemical and Biochemical Analysis Systems (Transducers Research Foundation, San Diego, California, USA, 2003), pp. 17–20.

E. Figallo, C. Cannizzaro, S. Gerecht, J.A. Burdick, R. Langer, N. Elvassore, G. Vunjak-Novakovic, Lab Chip **7**, 710–719 (2007)

P. Gadue, T.L. Huber, M.C. Nostro, S. Kattaman, G.M. Keller, Exp. Hematol. **33**, 955–964 (2005)

B.M. Johansson, M.V. Wiles, Mol. Cell. Biol. **15**, 141–151 (1995)

L. Kim, M.D. Vahey, H. Lee, J. Voldman, Lab Chip **6**, 394–406 (2006)

H. Kimura, T. Yamamoto, H. Sakai, Y. Sakai, T. Fujii, Lab Chip **8**, 741–746 (2008)

N. Korin, A. Bransky, U. Dinnar, S. Levenberg, Biomed. Microdev. **11**, 87–94 (2009)

T. Kunath, M.K. Saba-El-Leil, M. Almousailleakh, J. Wray, S. Meloche, A. Smith, Development **134**, 2895–2902 (2007)

D.A.F. Loebel, C.M. Watson, R.A.D. Young, P.P.L. Tam, Dev. Biol. **264**, 1–14 (2003)

S. Masui, S. Ohtsuka, R. Yagi, K. Takahashi, M.S. Ko, H. Niwa, BMC Dev. Biol. **8**, 45 (2008)

I. Meyvantsson, D.J. Beebe, Annu. Rev. Anal. Chem. **1**, 141–1427 (2008)

N.D. Miljkovic, G.M. Cooper, K.G. Marra, Osteoarthritis Cartilage **16**, 1121–1130 (2008)

M. Mohammadi, Science **276**, 955 (1997)

J.C. Mohr, J.J. de Pablo, S.P. Palecek, Biomaterials **27**, 6032–6042 (2006)

C.E. Murry, G. Keller, Cell **132**, 661–680 (2008)

A. Nagy, M. Gertsenstein, K. Vintersten, R. Behringer, *Manipulating the Mouse Embryo A Laboratory Manual*, 3rd edn. (Cold Spring Harbor, New York, 2003), pp. 32–38

H. Niwa, Development **134**, 635–646 (2007)

H. Niwa, J. Miyazaki, A.G. Smith, Nat. Genet. **24**, 372–376 (2000)

S. Ogawa, Y. Tagawa, A. Kamiyoshi, A. Suzuki, J. Nakayama, Y. Hashikura, S. Miyagawa, Stem Cells **23**, 903–913 (2005)

L. Palmqvist, C.H. Glover, L. Hsu, M. Lu, B. Bossen, J.M. Piret, R.K. Humphries, C.D. Helgason, Stem Cells **23**, 663–680 (2005)

J. M. Ruijter, C. Ramakers, W. M. H. Hoogaars, Y. Karlen, O. Bakker, M. J. B. van den Hoff, A. F. M. Moorman, Nucleic Acids Res. (2009) doi:10.1093/nar/gkp045

A.M. Singh, N. Terada, Trends Cardiovasc. Med. **17**, 96–101 (2007)

A.G. Smith, Annu. Rev. Cell Dev. Biol. **17**, 435–462 (2001)

W.C. Smith, R.M. Harland, Cell **70**, 829–840 (1992)

T. Teratani, H. Yamamoto, K. Aoyagi, H. Sasaki, A. Asari, G. Quinn, H. Sasaki, M. Terada, T. Ochiya, Hepatology **41**, 836–846 (2005)

S. Vainio, I. Karavanova, A. Jowett, I. Thesleff, Cell **75**, 45–58 (1993)

G.M. Walker, H.C. Zeringue, D.J. Beebe, Lab Chip **4**, 91–97 (2004)

M. V. Wiles, G. Proetzel, in *Embryonic Stem cells A Practical Approach*, ed. by E. Notarianni, M.J. Evans (Oxford University Press, New York, 2006), pp. 112–119

Q.L. Ying, J. Nichols, I. Chambers, A. Smith, Cell **115**, 281–292 (2003a)

Q.L. Ying, M. Stavridis, D. Griffiths, M. Li, A. Smith, Nat. Biotechnol. **21**, 183–186 (2003b)

Q.L. Ying, J. Wray, J. Nichols, L. Batlle-Morera, B. Doble, J. Woodgett, P. Cohen, A. Smith, Nature **453**, 519–524 (2008)

H. Yu, I. Meyvantsson, I.A. Shkel, D.J. Beebe, Lab Chip **5**, 1089–1095 (2005)

original article

MT Open

Efficient Generation of Hepatoblasts From Human ES Cells and iPS Cells by Transient Overexpression of Homeobox Gene *HEX*

Mitsuru Inamura[1,2], Kenji Kawabata[2,3], Kazuo Takayama[1,2], Katsuhisa Tashiro[2], Fuminori Sakurai[2], Kazufumi Katayama[1,2], Masashi Toyoda[4], Hidenori Akutsu[4], Yoshitaka Miyagawa[5], Hajime Okita[5], Nobutaka Kiyokawa[5], Akihiro Umezawa[4], Takao Hayakawa[6,7], Miho K Furue[8,9] and Hiroyuki Mizuguchi[1,2]

[1]Department of Biochemistry and Molecular Biology, Graduate School of Pharmaceutical Sciences, Osaka University, Osaka, Japan; [2]Laboratory of Stem Cell Regulation, National Institute of Biomedical Innovation, Osaka, Japan; [3]Department of Biomedical Innovation, Graduate School of Pharmaceutical Science, Osaka University, Osaka, Japan; [4]Department of Reproductive Biology, National Institute for Child Health and Development, Tokyo, Japan; [5]Department of Developmental Biology and Pathology, National Institute for Child Health and Development, Tokyo, Japan; [6]Pharmaceutics and Medical Devices Agency, Tokyo, Japan; [7]Pharmaceutical Research and Technology Institute, Kinki University, Osaka, Japan; [8]JCRB Cell Bank/Laboratory of Cell Culture, Department of Disease Bioresource, National Institute of Biomedical Innovation, Osaka, Japan; [9]Laboratory of Cell Processing, Institute for Frontier Medical Sciences, Kyoto University, Kyoto, Japan

Human embryonic stem cells (ESCs) and induced pluripotent stem cells (iPSCs) have the potential to differentiate into all cell lineages, including hepatocytes, *in vitro*. Induced hepatocytes have a wide range of potential application in biomedical research, drug discovery, and the treatment of liver disease. However, the existing protocols for hepatic differentiation of PSCs are not very efficient. In this study, we developed an efficient method to induce hepatoblasts, which are progenitors of hepatocytes, from human ESCs and iPSCs by overexpression of the *HEX* gene, which is a homeotic gene and also essential for hepatic differentiation, using a HEX-expressing adenovirus (Ad) vector under serum/feeder cell-free chemically defined conditions. Ad-HEX-transduced cells expressed α-fetoprotein (AFP) at day 9 and then expressed albumin (ALB) at day 12. Furthermore, the Ad-HEX-transduced cells derived from human iPSCs also produced several cytochrome P450 (CYP) isozymes, and these P450 isozymes were capable of converting the substrates to metabolites and responding to the chemical stimulation. Our differentiation protocol using Ad vector-mediated transient HEX transduction under chemically defined conditions efficiently generates hepatoblasts from human ESCs and iPSCs. Thus, our methods would be useful for not only drug screening but also therapeutic applications.

Received 18 March 2010; accepted 13 October 2010; published online 23 November 2010. doi:10.1038/mt.2010.241

INTRODUCTION

Human embryonic stem cells (ESCs) and induced pluripotent stem cells (iPSCs) are able to replicate indefinitely and differentiate into most cell types of the body,[1–4] and thereby have the potential to provide an unlimited source of cells for a variety of applications.[5] Hepatocytes are useful cells for biomedical research, regenerative medicine, and drug discovery. They are particularly applicable to drug screenings, such as for the determination of metabolic and toxicological properties of drug compounds in *in vitro* models, because the liver is the main detoxification organ in the body.[6] For these applications, it is necessary to prepare a large number of functional hepatocytes from human ESCs and iPSCs. Many of the existing methods for cell differentiation of human ESCs and iPSCs into hepatocytes employ undefined, serum-containing medium and feeder cells.[7–9] Preparation of human ESC- and iPSC-derived hepatocytes for therapeutic applications and drug toxicity testing in humans should be done in nonxenogenic culture systems to avoid potential contamination with pathogens. Furthermore, the efficiency of the differentiation of the human ESCs and iPSCs into hepatocytes is not particularly high using these methods.[9–14]

In vertebrate development, the liver is derived from the primitive gut tube, which is formed by a flat sheet of cells called the definitive endoderm.[5,15] Shortly afterwards, the definitive endoderm is separated into endoderm derivatives containing the liver bud, the cells of which are referred to as hepatoblasts. The hepatoblasts have the potential to proliferate and differentiate into both hepatocytes and cholangiocytes. In the process of hepatic differentiation, the maturation is characterized by the expression of liver- and stage-specific genes. For example, α-fetoprotein (AFP) is an early hepatic marker, which is expressed in hepatoblasts in the liver bud until birth, and its expression is dramatically reduced after birth.[16] In contrast, albumin (ALB), which is the most abundant protein synthesized by hepatocytes, is initially expressed at lower levels in early fetal hepatocytes, but its expression level is increased as the hepatocytes mature, reaching a maximum in adult hepatocytes.[17] Furthermore, isoforms of cytochrome P450 (CYP) proteins also exhibit differential expression levels according to the developmental stages

Correspondence: *Hiroyuki Mizuguchi, Department of Biochemistry and Molecular Biology, Graduate School of Pharmaceutical Sciences, Osaka University, 1-6 Yamadaoka, Suita, Osaka 565-0871, Japan. E-mail: mizuguch@phs.osaka-u.ac.jp*

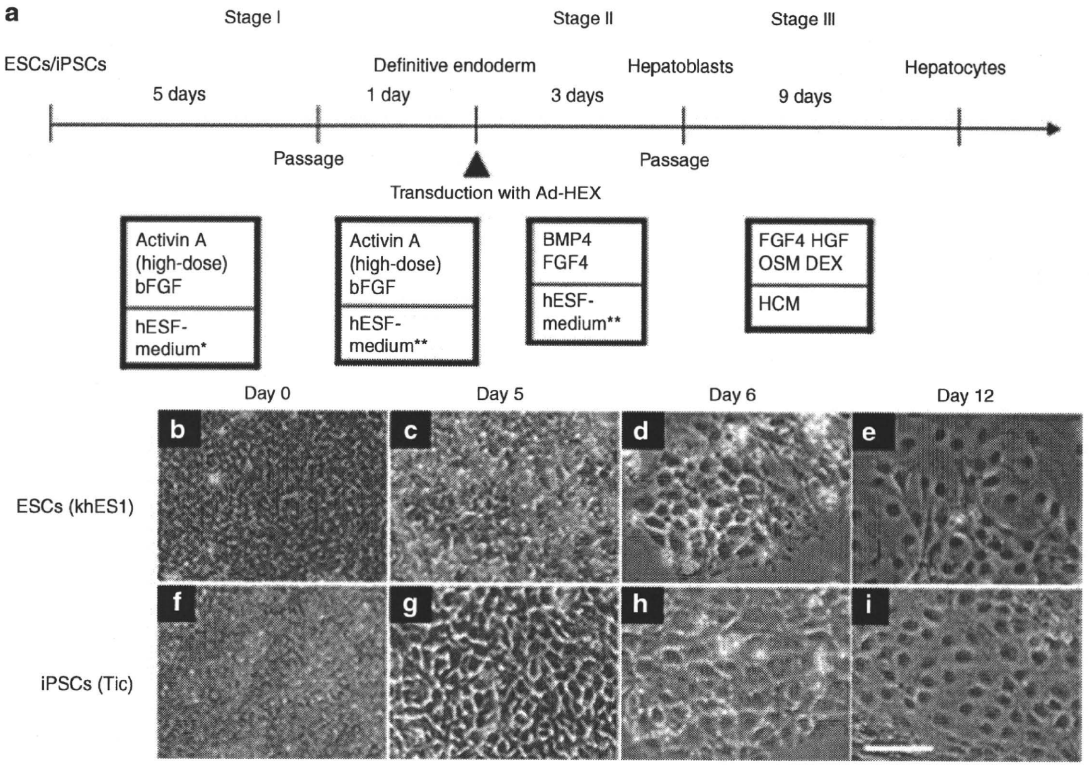

Figure 1 A strategy of differentiation of human embryonic stem cells (ESCs) and induced pluripotent stem cells (iPSCs) to hepatoblasts and hepatocytes. (**a**) Schematic representation illustrating the procedure for differentiation of human ESCs (khES1) and iPSCs (Tic) to hepatocytes. (**b–i**) Phase contrast microscopy showing sequential morphological changes (day 0–12) from (**b–e**) human ESCs (khES1) and (**f–i**) iPSCs (Tic) to hepatoblasts via the definitive endoderm. Bar = 50 μm. bFGF, basic fibroblast growth factor; BMP4, bone morphogenetic protein 4; DEX, dexamethasone; FGF4, fibroblast growth factor 4; HGF, hepatocyte growth factor; OSM, Oncostatin M; HCM, hepatocytes culture medium; *, hESF-GRO medium that was supplemented with 10 μg/ml human recombinant insulin, 5 μg/ml human apotransferrin, 10 μmol/l 2-mercaptoethanol, 10 μmol/l ethanolamine, 10 μmol/l sodium selenite, 0.5 mg/ml fatty acid free BSA; **, hESF-DIF medium that was supplemented with 10 μg/ml insulin, 5 μg/ml apotransferrin, 10 μmol/l 2-mercaptoethanol, 10 μmol/l ethanolamine, 10 μmol/l sodium selenite, 0.5 mg/ml BSA.

of the liver. Although most CYPs (including CYP3A4, CYP7A1, and CYP2D6) are only slightly expressed or not detected in the fetal liver tissue, the expression levels are dramatically increased after birth.[18]

For the development of hepatoblasts, numerous transcription factors are required, such as hematopoietically expressed homeobox (*HEX*), GATA-binding protein 6, prospero homeobox 1, and hepatocyte nuclear factor 4A.[15,19] Among them, *HEX* is suggested to function at the earliest stage of hepatic linage.[20] HEX is first expressed in the definitive endoderm and becomes restricted to the future hepatoblasts. Targeted deletion of the *HEX* gene in the mouse results in embryonic lethality and a dramatic loss of the fetal liver parenchyma.[19,21,22] The hepatic genes, including *ALB*, prospero homeobox1, and hepatocyte nuclear factor 4A, are transiently expressed in the definitive endoderm of *HEX*-null embryos, and further morphogenesis of the hepatoblasts does not occur.[23] In general, then, *HEX* is essential for the definitive endoderm to adopt a hepatic cell fate.

Adenovirus (Ad) vectors are one of the most efficient gene delivery vehicles and have been widely used in both experimental studies and clinical trials.[24] Ad vectors are attractive vehicles for gene transfer because they are easily constructed, can be prepared in high titers, and provide high transduction efficiency in both dividing and nondividing cells. We have developed efficient methods for Ad vector-mediated transient transduction into mouse ESCs and iPSCs.[25,26] We have also showed that the differentiations of mouse ESCs and iPSCs into adipocytes and osteoblasts were dramatically promoted by Ad vector-mediated peroxisome proliferator activated receptor γ and runt related transcription factor 2 transduction, respectively.[25,26]

In this study, we hypothesized that transient *HEX* transduction could efficiently induce hepatoblasts from human ESCs and iPSCs. A previous study demonstrated that *HEX* regulates the differentiation of hemangioblasts and endothelial cells from mouse ESCs,[27] whereas the role of *HEX* in the differentiation of hepatoblasts from human ESCs and iPSCs remains unknown. We found that differentiation of hepatoblasts from the human ESC- and iPSC-derived definitive endoderms, but not from undifferentiated human ESCs and iPSCs, could be facilitated by Ad vector-mediated transient transduction of a *HEX* gene. Furthermore, the Ad-HEX-transduced cells that were derived from human iPSCs were able to differentiate into functional hepatocytes *in vitro*. All the processes for cellular differentiation were performed under serum/feeder cell- free chemically defined conditions. Our culture systems and differentiation method based on Ad vector-mediated transient transduction under chemically defined conditions would provide a platform for drug screening as well as safe therapies.

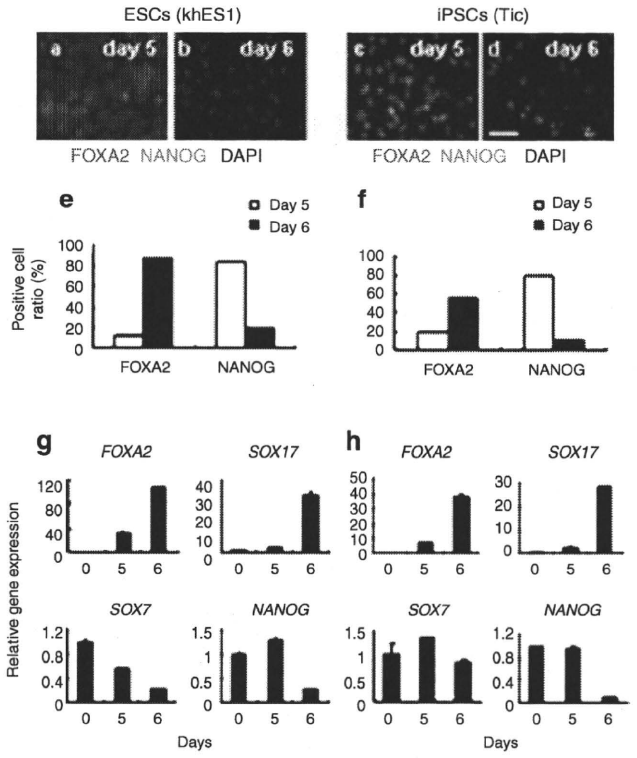

Figure 2 Characterization of the human ESC (khES1)- and iPSC (Tic) derived definitive endoderms. (**a–d**) The immunofluorescent staining of the human ESC (khES1)- and iPSC (Tic) derived differentiated cells before (**a** and **c**; day 5) and after passaging (**b** and **d**; day 6). The cells were immunostained with antibodies against FOXA2 and NANOG. Nuclei were stained with DAPI. (**e**,**f**) Semiquantitative analysis of the immunofluorescent staining in **a–d**. Data are presented as the mean of immunopositive cells counted in eight independent fields. (**g**,**h**) Real-time RT-PCR analysis of the level of definitive endoderm (*FOXA2* and *SOX17*), pluripotent (*NANOG*), and extra-embryonic endoderm (*SOX7*) gene expression at day 5 and 6. At day 5, the cells were passaged. Therefore, the data at day 5 and 6 show the levels of gene expression before (at day 5) or after the passage (at day 6). Data are presented as the mean ± SD from triplicate experiments. The graphs represent the relative gene expression level when the level of undifferentiated cells at day 0 was taken as 1. Bar = 50μm. ESC, embryonic stem cells; iPSC, induced pluripotent stem cells.

RESULTS

Differentiation of human ESC- and iPSC-derived definitive endoderms

Our three-step differentiation protocol is illustrated in **Figure 1a**. After treatment with 50 ng/ml of Activin A (high-dose) and basic fibroblast growth factor (bFGF) for 5 days on a laminin-coated plate, morphologically, the human ESCs and iPSCs were gradually transformed from typical, defined, tight human ESC, and iPSC colonies (day 0) into less dense, flatter cells containing prominent nuclei (day 5), even though the majority of the cells had a morphology resembling that of undifferentiated cells (**Figure 1b,c,f,g**). FACS analysis showed that ~46% of human iPSC-derived differentiated cells expressed CXCR4 (expressed in the definitive endoderm but not the primitive endoderm) (**Supplementary Figure S1a**). Human ESC- and iPSC-derived differentiated cells were immunostained with the definitive endoderm marker, FOXA2 (**Figure 2a,c**). However, the majority of the cells expressed the pluripotent marker NANOG, indicating that undifferentiated cells remain in the induced cultures at day 5. After the cells were passaged with trypsin-EDTA and seeded on a laminin-coated plate a second time, the resultant cells were found to be more homogeneous and flatter at day 6 (**Figure 1d,h**). Semiquantitative analysis by counting immunopositive cells revealed that the number of FOXA2-positive cells was increased and, in turn, the number of NANOG-positive cells was decreased at day 6 after passaging (**Figure 2e,f**). Real-time reverse transcriptase (RT)-PCR analysis showed that the definitive endoderm markers *FOXA2* and *SOX17* mRNA were upregulated, whereas the pluripotent marker *NANOG* mRNA was downregulated at day 6 (**Figure 2g,h**). These results were consistent with the immunofluorescence results (**Figure 2a–d**). The expression levels of the mesoderm marker *FLK1* mRNA and ectoderm marker *PAX6* mRNA were downregulated or unchanged at day 6 (**Supplementary Figure S1b–e**). Importantly, the expression of *SOX7* mRNA (expressed in the extra-embryonic endoderm but not the definitive endoderm) was downregulated (**Figure 2g,h**). These results indicate that the definitive endoderm is induced or selected from human ESCs and iPSCs after passaging. We obtained the same results using another human iPSC line (**Supplementary Figure S2a–d**).

HEX induces hepatoblasts from the human ESC- and iPSC-derived definitive endoderms

To investigate whether forced expression of transcription factors could promote hepatic differentiation, the human ESC- and iPSC-derived definitive endoderms were transduced with Ad vectors. We used a fiber-modified Ad vector containing the elongation factor-1α promoter and a stretch of lysine residue (K7) peptides in the C-terminal region of the fiber knob to examine the transduction efficiency in the human ESC- and iPSC-derived definitive endoderms. The elongation factor-1α promoter was found to be highly active in human ESCs.[28] The K7 peptide targets heparan sulfates on the cellular surface, and the fiber-modified Ad vector containing K7 peptides was shown to be efficient for transduction into many kinds of cells.[29,30] The human ESC- and iPSC-derived definitive endoderms were transduced with a LacZ-expressing Ad vector (Ad-LacZ) at 3,000 vector particle/cell. X-Gal staining showed that the Ad-LacZ-transduced human ESC- and iPSC-derived definitive endoderms successfully expressed LacZ (**Figure 3**). Nearly 100% of the cells transduced with Ad-LacZ were strongly X-gal positive. The transduction efficiency in the human ESC- and iPSC-derived definitive endoderms transduced with the conventional Ad vector containing the wild-type capsid at 3,000 vector particle/cell was ~80% and X-gal staining was much weaker than that in the cells transduced with fiber-modified Ad vectors (**Supplementary Figure S6**).

Next, the human ESC- and iPSC-derived definitive endoderms were transduced with a HEX-expressing fiber-modified Ad vector (Ad-HEX). Although HEX is known to be a transcription factor that is essential for liver development, it remains unclear what the effect of transient *HEX* overexpression is on differentiation from human ESCs and iPSCs or their derivatives *in vitro*. We confirmed the overexpression of *HEX* in the human ESC- and iPSC-derived definitive endoderms transduced with Ad-HEX (**Supplementary Figure S3a–f**). Gene expression analysis revealed the upregulation of *AFP* mRNA, which was expressed by hepatoblasts or early hepatocytes, in Ad-HEX-transduced cells as